UNIVERSITÀ DEGLI STUDI DI PADOVA
DIPARTIMENTO DI INGEGNERIA INDUSTRIALE

TESI DI LAUREA MAGISTRALE IN INGEGNERIA CHIMICA E DEI PROCESSI INDUSTRIALI

A LAB-ON-A-CHIP SYSTEM FOR CELL MICROENCAPSULATION IN A POLYMERIC MATERIAL

Relatore: Ing. Nicola Elvassore
Correlatore: Ing. Tommy Haraldsson

Laureanda: SILVIA PICCOLI

ANNO ACCADEMICO 2011 – 2012

Tutte le verità sono facili da capire una volta che sono state rivelate.
Il difficile è scoprirle...

All truths are easy to understand once they are discovered;
the point is to discover them...

Galileo Galilei (1564 - 1642)

Abstract

In order to give a concrete response to the need of novel drug delivery systems for cancer treatment, a microfluidic device designed for cell encapsulation has been developed in this thesis work. Water in oil (w/o) and oil in water (o/w) emulsion processes are carried out in the microsystems produced during the thesis project, which is the start point for encapsulating cells.

Specific microfabrication techniques are employed in the development of the microchip, made using a novel polymeric platform, called Off-Stoichiometry Thiol-Ene/Epoxy (OSTE (+)).

The microsystem is tested to verify the features needed for the application desired; hydrophobic surface properties, good bonding properties and no clogging in the channels are shown.

After connecting the microchip to a proper pumping system through a ″chip-to-world″ connection, experimental analysis are conducted to understand how the volumetric flow rates of the fluids employed influence the size of the droplets generated, their frequency of production and the regimes of flow in the microchannels. Furthermore, droplet generation dependence on microfluidic channels geometries is investigated. The emulsion processes are observed through an optical microscope and a digital camera.

The experimental results show how a high value of the flow rate ratio between the continuous phase and the dispersed phase, for both w/o and o/w emulsions, allows for high production frequency of droplets with size comparable to the channel's width, as required for an emulsion process whose aim is cell encapsulation. Moreover the tests conducted highlight that the innovative polymeric material employed and the microfluidic device fabricated both are suited for the development of a new drug delivery system through encapsulation of artificial cells.

With further validation on polyethylene glycol (PEG) instead of water, the developed device will be a useful tool for double emulsion processes for cell encapsulation.

Riassunto

Questo lavoro di tesi tratta dello sviluppo di una piattaforma microfluidica dove verranno condotti dei processi di emulsione al fine di ottenere delle gocce di acqua in olio minerale e delle gocce di olio minerale in acqua.
Specifiche tecniche di microfabbricazione sono impiegate per lo sviluppo del microchip, costituito da un nuova piattaforma polimerica, chiamata *Off-Stoichiometry Thiol-Ene/Epoxy* (OSTE (+)).
Il microsistema viene testato al fine di verificare che soddisfi le caratteristiche richieste per l'applicazione desiderata; in particolare si dimostra la presenza di proprietà superficiali idrofobiche, perfetta adesione tra i due strati che formano lo strumento e assenza di ostruzioni nei canali.
Dopo aver connesso il microchip con un apposito sistema di pompaggio, alcune prove sperimentali vengono condotte al fine di determinare l'influenza delle portate volumetriche dei fluidi utilizzati sulle dimensioni delle gocce generate, sulla loro frequenza di produzione e sui regimi di flusso instaurati. Geometrie diverse dei canali microfluidici sono inoltre esaminate. Le analisi vengono condotte tramite un microscopio ottico e una fotocamera digitale.
I risultati delle prove sperimentali dimostrano come un valore elevato del rapporto tra la portata volumetrica della fase continua e quello della fase dispersa permetta di ottenere un'alta frequenza di gocce di dimensioni comparabili a quelle dei canali, requisito necessario per un processo di emulsione finalizzato a incapsulare cellule. Inoltre dalle prove condotte emerge come l'innovativo materiale polimerico impiegato e lo strumento microfluidico fabbricato siano adatti per lo sviluppo di un nuovo sistema di rilascio di farmaci nel corpo tramite l'incapsulazione di cellule artificiali.
Ulteriori analisi sperimentali che impiegano glicole polietilenico (PEG) invece di acqua sono necessarie per poter poi impiegare il microchip progettato e fabbricato in processi di emulsione per incapsulare cellule.

Table of content

Introduction

Cell microencapsulation technology requires materials with proper porosity and hydrophilic properties, in order to maintain the cells alive and to produce therapeutic proteins. The encapsulation can be carried out in a microfluidic device through a double emulsion process, since it allows for a precise control of the beads formed. The design, the material used and the fabrication of the microsystem should enable a device with good mechanical, bonding and surface properties.

In this thesis work a microfluidic platform for emulsion processes was developed and tested. The microfluidic device was fabricated using a novel polymeric material, called Off-Stoichiometry Thiol-Ene/Epoxy (OSTE (+)). The microsystem was used for a high frequency production of both water in oil (w/o) and oil in water (o/w) droplets. Making droplets implies a good control of the flow rates of the immiscible fluids employed, of their properties, especially the viscosity, and their interfacial tension.

This work is the starting point of a project called TheraCage, which involve Karolinska Institute and Polymer MEMS (KTH - Microsystem Technology Lab), whose purpose is to develop a new therapeutic technology for the treatment of medulloblastoma and neuroblastoma, which are brain' tumors that particularly afflict children. The new therapy method uses transfected cells as a novel drug delivery vehicle, implanted into the tumor via a blood vessel which enables subjecting the tumor site to very high doses of a cytostatic drug. This novel cell-based treatment will allow for a precise control of the therapeutic cells through a polymer encapsulation, generated in the microfluidic device fabricated during this thesis work.

In Chapter 1 the importance of cell microencapsulation and its applications are treated; the materials and the processes typically used for encapsulating the cells are presented. Then the advantages of using microfluidic devices in the biomedical field are highlighted and the new materials Off-Stoichiometry Thiol-Ene (OSTE) and Off-Stoichiometry Thiol-Ene/Epoxy (OSTE (+)) are described as alternative material to the polydimethylsiloxane (PDMS), commonly used in microfluidic applications. Finally the aim and the objectives of this thesis are explained.

In Chapter 2 the fabrication methods of the microfluidic device, the equipment and the materials employed are described. The focus is on the following microfabrication techniques: photolithography, PMDS molding process, OSTE (+) mixing, casting and back-end processes.

In Chapter 3 the characterization's methods carried out on the microdevice fabricated are described. The tests conducted are contact angle measurement, flow tests and bonding tests.

For each test the method of measurement, the setup needed and the results achieved are described in some detail.
In Chapter 4 the structure and the development of the microfluidic platform to get droplets are described; different geometrical configurations of the microfluidic device are investigated. The setup for the experiments, how to connect the device to the macro world and the experimental analysis conducted are explained. Experimental results are reported and discussed for both water in oil and oil in water emulsions.

Chapter 1

Introduction and background

The present Master thesis work was carried out at the ″Department of Electrical Engineering″ of ″Royal Institute of Technology - KTH″ in Stockholm, Sweden. In this department, inside the ″Division of Microsystem Technology - MST″ there is the ″OSTE research group″ directed by Dr. Tommy Haraldsson. At this group, the thesis work was developed from March to September 2012, with the supervision of Dr. Haraldsson.
This first chapter deals with the importance of cell microencapsulation and of its applications; there will be underlined the materials and the processes commonly used to encapsulate the cells.
Then it will focus on the advantages of using microfluidic devices in the biomedical field and the new material Off-Stoichiometry Thiol-Ene (OSTE) will be described as an alternative material to the polydimethylsiloxane (PDMS), commonly used in microfluidic applications.

1.1 Cell encapsulation

Cell encapsulation (Figure 1.1) represents a technique that has been around for many years, but while experience in preclinical animal models is broad, clinical applications are sparse; some examples of use of this technology are in treatment of diabetes, anemia, hemophilia, renal failure and hypoparathyroidism (*Orive et al.*, 2003).

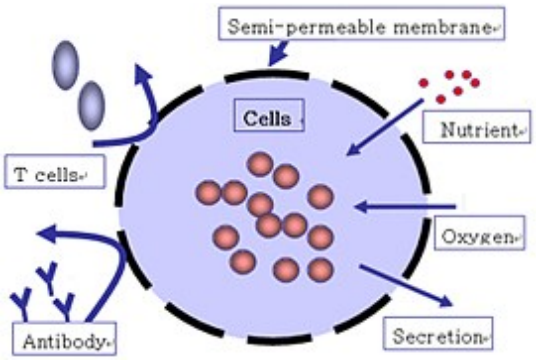

Figure 1.1. *Encapsulation of cells. Figure from Madame Curie bioscience database.*

The concept of putting drugs into a sphere is a quite old idea, explained for the first time at the turn of the 20th century by Paul Ehrlich, who coined the term ″magic bullets″ (*Witkop*,

1999). ″Magic bullets″ were supposed to be antibodies, microspheres or capsules containing cells; an example of encapsulation of drugs is shown in Figure 1.2.

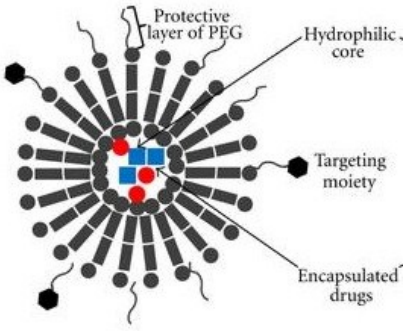

Figure 1.2. *Encapsulation of drugs. Figure from Madame Curie bioscience database.*

Some years later, in the fifties, the idea of encapsulating living cells for therapeutic use was proposed by Chang and its first application had been the encapsulation of islet cells to treat diabetes (*Chang*, 1957). In 1964, he also proposed the use of ultrathin polymer membrane microcapsules for the immunoprotection of transplanted cells and he introduced the term ″artificial cells″ to describe the concept of bioencapsulation, which was successfully implemented 20 years later in the immobilization of xenograft islet cells.

Cell microencapsulation technology is based on the immobilization of cells inside a semipermeable material. The outside material shelters the encapsulated and trapped cells from both mechanical stress and the host's immune system, while it allows the bidirectional diffusion of nutrients, oxygen, and waste, needed to keep the cells alive (*Murua et al*., 2008). On the other side, encapsulation of cells also protects the host from these genetically modified cells. This ability to protect foreign cells, to prevent premature destruction and to provide containment for the cells makes this technology very attractive.

The main advantages of cell encapsulation for drug delivery applications are the elimination of immunosuppression, which is the barrier against foreign and even genetically modified cells, and the continuous delivery of a therapeutic substance for a prolonged period of time. Furthermore drug encapsulation can improve drug solubility and stability, can reduce drug resistance in some human carcinomas, so that the efficacy and the security of the therapy will be enhanced. In particular in cancer treatment this kind of delivery system avoids or at least reduces some disadvantages of chemotherapy: toxicity, pain management and repeated administrations (*Allen and Cullis*, 2004), in order to improve the quality of patients' lives. This new technology has the potential to be effective in eradicating cancer and it should, at the very least, make the disease's treatment less painful and less invasive than standard chemotherapy.

Using encapsulation, the drugs can be released at the right time, in the target where it is needed and at the level that is required, so that the full potential of therapeutic molecules is

realized (*Orive et al.*, 2005). Encapsulated cells can be delivered by different routes into the body: oral, intravenous, intra-arterial, intra-peritoneal or direct injection into the tissue or tumor.

Researches on this technology have been conducted by Robert Langer and other researches at MIT (Massachusetts Institute of Technology – Cambridge, USA). They have focused on the controlled release of drugs to determine if a microfluidic platform could work as a pulsatile drug delivery system, commonly used to treat people with diseases that need drugs to be delivered at different rates over time. They discovered that the storage and the on-demand delivery of drugs can be reached by a microfluidic cell encapsulation technology. Other studies have been carried out in the field of ambulatory emergency care treatment, and systems to rapidly deliver drugs in emergency situations have been developed (*Elman et al.*, 2009).

The main problem of all cell therapies involving the transfer of living cells is the trend of the cells to proliferate and divide (*Williams et al.*, 1999), since their containment can be cracked or broken. Therefore cells can grow beyond the transplantation site and form tumors (*Hoffman et al.*, 1993).

The clinical use of cell encapsulation requires some important standards, which regard to the biocompatibility of encapsulating material, the contamination problem during preparations process and the viability of the encapsulated cells, which needs the transport of macromolecules across the interface. These features can be improved by co-application of suitable polymeric matrices and growth factors and by the determination of the right pore size of the matrices.

1.1.1 Materials for cell encapsulation

There are many requirements for the material used for the microbeads' core, such as high biocompatibility (no inflammatory or toxic responses when placed in contact with the cells and when implanted in vivo), suitable durability, selective transport of molecules (appropriate permeability), mechanical, chemical and thermal stability and it has to be easily sterilized prior to cell addition and metabolized in the body without the formation of toxic metabolites.

Both synthetic and natural polymers can be used for cell encapsulation; for that application they have to be biodegradable, plastic and adaptable to various situations.

The main features of the material that have to be considered are its porosity and its hydrophilic properties. A good material should allow the quality control of the encapsulated cells from the point of view of the vitality and of the production of therapeutic proteins.

1.1.1.1 Polyethylene glycol (PEG)

Among different synthetic polymer, polyethylene glycol (PEG) is one the most used in pharmaceutical and biomedical applications. It is composed of repeating C-C-O sequences (Figure 1.3) of specified length.

Figure 1.3. *Repeating unit of polyethylene glycol (PEG).Figure from Chemfinder.com.*

The terminal groups are initially hydroxyls, though these can be replaced with polymerizable acrylate groups prior to crosslinking. To encapsulate cells with PEG a solution of the acrylated polymer (PEGDA, Figure 1.4), a photoinitiator and the cells have to be exposed to light of specific wavelengths, hereby the photocrosslinking of the PEG capsule occurs and the cells will be suspended into a hydrogel.

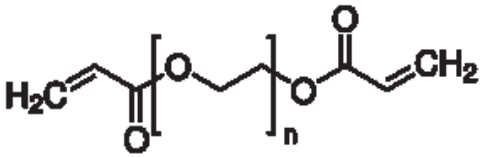

Figure 1.4. *Repeating unit of polyethylene glycol diacrylate (PEGDA).Figure from SigmaAldrich.com.*

Some advantages of using PEG are its intrinsic ability to minimize protein adsorption, which consequently reduces fibroblast overgrowth, and its synthetic nature, which guarantees a good reproducibility in results. PEG can be controlled within the laboratory and changing parameters such as concentration, molecular weight and degree of functionalization allows for manipulation of polymer properties according to specific applications. PEG-based materials are non-toxic, robust, with inert properties and they can produce a hydrophilic polymer used as biocompatible hydrogel. Moreover with the use of PEG the issue of source variability that plagues natural polymers is overcome. For these reasons this polymer has become popular in the biomedical field and some examples of applications are cell encapsulation, micro arrays of cells, drug delivery and tissue engineering.

The main drawbacks of PEG's use are due to its rapid chemical polymerization, which may clogs the microchannels of the device and minimal protein adsorption, which can be an obstacle to cell adhesion. To avoid this issue PEG should be modified, but then more complexity is added to the encapsulating process, since PEG's modifications are time consuming and costly.

1.1.1.2 Synthetic materials

Others polymers commonly used for cell microencapsulations are cellulose sulphate-based materials (NaCS), polyethersulfone, polyacrylnitrile and hyaluronic acid.

NaCS-based materials present high mechanical stability, quick production procedure, they allow secretion of large molecules (*Löhr et al.,* 2001) and they cause a limited immune response and no reactions in the host body. The major drawbacks of the NaCS-based encapsulation system are the lack of toxicological data, the fact the material has to be synthetized under controlled conditions and is difficult to handle.
Polyethersulfone has good hydrophilic properties, is available in a variety of pore sizes, is rigid, with high mechanical strength and stability, but not resistant to polar organic solvents and aromatic hydrocarbons.
Polyacrylnitrile is remarkable for its thermal stability and its resistance to many organic solvents.
Several studies have been conducted on hyaluronic acid (HA) as an encapsulating material, for its numerous natural functions, physical properties and high biocompatibility (*Hahn et al.,* 2004). HA is a natural, linear, and negatively charged polysaccharide, composed of disaccharide repeat units of D-glucuronic acid and N-acetyl-D-glucosamine (Figure 1.5).

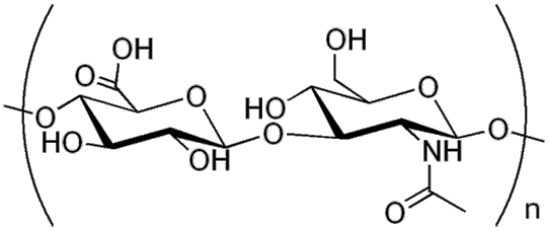

Figure 1.5. *Hyaluronic acid. Figure from Hahn, et al., 2004.*

Intracellular HA can be used for many fundamental functions, like the supply of cell migration, growth and differentiation of cells, and the help in wound repair. When uncrosslinked, soluble HA presents limited mechanical properties and degrades rapidly, but chemical modifications or photocrosslinking can form HA hydrogels and improve these features. Chemical change usually involves the carboxyl or hydroxyl groups of the HA backbone: the carboxylic acid groups can be modified with methacrylamide, while the alcohol groups can react with divinyl sulfone and diglycidyl ethers (*Segura et al.*, 2005).
Hyaluronic acid seems to be a suitable material for encapsulating cells because it is naturally derived, nonimmunogenic and bioactive; furthermore it has recently been shown that HA-composite hydrogels are hydrated, pliable and allow a controlled release of a model protein (*Leach et al.*, 2005). Disadvantages are mainly its limited mechanical strength and its fast enzymatic degradation by hyaluronidase.

1.1.1.3 Natural polymers

Biomaterials can also be used for cell encapsulation and some examples are: -collagene, whose main features are high cost to purify, natural variability and variation in enzymatic

degradation, depending on the location and state of the implant site;- chitosan, with weak mechanical properties and lack of bioactivity;- agarose.

However the most used natural polymer is alginate with poly-L-lysine (PLL). Alginate consists of a biopolymer which comes from natural growing algae. It is a naturally derived linear polysaccharide consisting of D-mannuronic acid (M-block) and R-L-guluronic acid (G-block) units, arranged in blocks rich in G units or M units and separated by blocks of alternating G and M units (Figure 1.6). The ratio of these two acids (G:M) influences several microcapsule properties, comprising mechanical strength and permeability (*De Groot et al*., 2003).

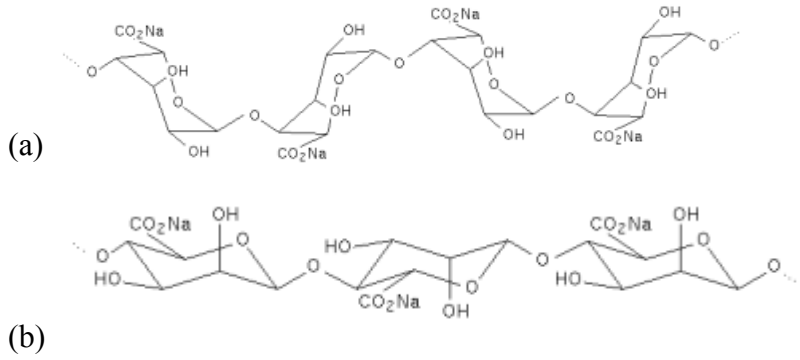

Figure 1.6. *Two repeating units of guluronic acid(a); two repeating units of mannuronic acid (b). Figure from http://www.cybercolloids.net/library/alginate/structure.php.*

The encapsulation procedure is quite complex: it involves the suspending of the cells of interest in a solution of alginate. In this aqueous solution, since alginate is polyanionic, it can be crosslinked by a divalent cation, such as Ca_2^+. Upon gelation of the alginate core, a layer of PLL (Figure 1.7), which is polycationic, is added and it is immediately bound to alginate. The gels are formed under very mild conditions by the reaction of the divalent cations with guluronic acid blocks in alginate; the gelation behavior is based on alginate's ability to bind these ions in a selective and cooperative way. Finally there is the reliquification of the capsule core carried out by an ion exchange which implies the substitution of Ca_2^+ ions with Na^+ ions.

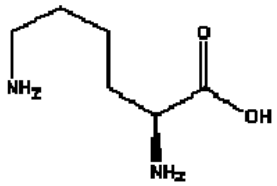

Figure 1.7. *Lysine structure. Figure from chemfinder.com.*

The process of alginate crosslinking and the following PLL layering are easy to conduct, but traces from the original material after the reliquification have to be avoided because they are

toxic and can cause an immunological response. However some clinical studies on the material have been conducted without safety problems.
Alginate with PLL passes nutrients, proteins, DNA and anticancer drugs, but blocks antibodies and immune cells. The use of alginate is favored since it is cheap, readily available, and cells immobilized in alginate gels keep a good viability during long-term culture thanks to the mild environment of the gel network. Its biocompatibility can only be achieved through sterilization and purification since it is a natural raw material, recovered from seaweed; these added process steps make the cost of the network preparation very high.
Another drawback of alginate's use is pyrogenicity, due to the pyrogenic or even toxic contaminants at ppm levels, that contaminate it and are very difficult to remove or to deactivate. Furthermore the main problem in using this material are the limited mechanical properties when ionically cross-linked with divalent cations: in fact the membrane is mechanically weak and alginate can affect the encapsulated cells in assay results; the hydrogels can also be disintegrated in an uncontrolled way. A solution could be the use of covalently cross-linked alginate with several polyethylene glycol (PEG) derivatives since the flexible PEG chains can provide elasticity to the system, while the stiff alginate chains provide mechanical strength to this two component system. A multicomponent system can offer versatility to the hydrogel in terms of degradation and mechanical properties. The properties of this system can be varied by changing its composition, the length of the cross-linking molecule or the cross-linking density as desired.
It should be also considered that a complete cell mass confinement is not guaranteed by this method of encapsulation with alginate.

1.2 Microfluidic devices in biomedical applications

Microfluidics refers to devices and methods for controlling and manipulating fluid flows with length scale less than a millimeter (*Stone et al.*, 2004). To realize microfluidic devices, operations have to be done on a miniaturized scale, in order to get the large-scale integration of functional components on a single monolithic device. The microelectronics industry was the first to develop miniaturized system, driven by the need to minimize costs by reducing the consumption of expensive reagents and by increasing throughput and automation.
Microfluidics is highly subject of studies for the following reasons:

- the availability of methods for fabricating individual and integrated flow configurations with length scales on the order of tens and hundreds of microns or smaller;

- manipulations of very small volumes (generally less than 1 microliter) and under the cellular length scale and also the ability to detect small quantities, in order to have great developments in the field of biology and biotechnology;
- the pursuit for cheap portable devices able to fulfill simple analytical tasks;
- the application of microsystems to perform fundamental researches in physical, chemical and biological processes;
- decreasing system size, sample size, response time, enabling massive parallelization and using convenient fabrication techniques.

Microfluidics can create ″chips″, which measure from only millimeters to a few centimeters in size and which contain integrated channels instead of circuits on glass or polymer substrates, with the purpose of making the fluids to flow, intermix and catalyze.

This technology is called Lab-On-a-Chip (LOC) and it has been developed from the Miniaturized Total Analysis System (μ-TAS), a concept introduced in 1990, according to which the entire analytical process, from sampling through detection, is integrated in a microfluidic system, in order to have faster analysis.

In the research field, microfluidic technologies have widely influenced various areas, especially in life sciences, including in-vitro diagnostics, drug discovery, biotechnology, and ecology. The LOC technology includes the development of point-of-care (POC) medical diagnostic devices, with the purpose of increasing sensitivity and having lower sample volumes, lower reagent volumes, low energy, low cost, low labor need and less likelihood of human error (*Xiao and Young*, 2011).

The field of research in microfluidics is increasing dramatically: in fact more than 30.000 papers have been published over the last 10 years on the topic (Web of Knowledge search using ‘microfluidic’ terms April 2012).

Many microfluidic products are already on the market and they have found a widespread use: pregnancy/ovulation tests, drugs of abuse tests, gene chips, devices for cardiac marker quantification and tests designed for bio-warfare protection.

The market of these devices is promising, it’s expected to grow at more than 20% in the next five years and to exceed $5B in 2016 (Yole Development market research, 2011). Drug discovery remains the first microfluidics market and it will continue to grow significantly as well. Commercial implementation in this area is more advanced than in the drug delivery area due to the complexity of sensing the concentration of the drug and controlling the release of new drug. The largest growth is expected in the field of point-of-care diagnostics, since today some products are moving from research applications to the clinical diagnostics and point of care fields (Figure 1.8); some examples could be the devices for diagnostics assays and biosensors. However, this trend is limited and the commercialization will be slower than what originally predicted due to the relative high manufacturing costs of many microfluidic devices

and to the fact that significant obstacles are still in the technology itself and in its fusion into the healthcare system.

Figure 1.8. *Molecular Vision's assay chip for polymer detection incorporating integrated organic photodiodes. Printed circuit board comprises amplifier and Bluetooth® connector for wireless data transfer to a PDA.*

1.2.1 Advantages and challenges for microfluidics

Compared to conventional macro-scale systems, microfluidic devices have many advantages: less reagent and sample consumption, reduced size and power requirement, low manufacturing costs, faster analysis, increased performance, high sample throughput, integration and automation possibilities, and disposability of portable analysis systems. Moreover microfluidic devices offer a superior and precise liquid control, the reaction environment in chemical reactions is well controlled and some reactions, impossible in the macro-world, can be carried out. For the small amount of waste generated it is also a 'green' technology.

However these devices present some drawbacks, such as handling of nanoscale volumes of liquids and the interfacing to the macro world. To obtain functional devices the following capacities are needed: a means of introducing reagents and samples, so called ″chip-to-world″ connections; methods for moving samples and reagents around the chip, and for merging and mixing fluid streams; various other components and unit operations such as sensors for microanalytical tasks, and components for purification and sample preparation.

Miniaturization is costly, design and fabrication are both difficult and expensive, and geometrical and surface chemistry issues have to be solved. Geometrical problem are potentially large capillary forces, possible evaporation and mixing performed only by diffusion, while surface chemistry concerns are clogging, blocking and adsorption of dissolved molecules.

Since many challenges are posed for microfluidic devices, the development of microfluidic systems is a multidisciplinary challenge, requiring knowledge not only in fluidics, micromachining, electro-magnetics, but also in materials, biology and chemistry.

1.2.2 Double emulsion process

An emulsion is a heterogeneous system consisting of at least one fluid, in the form of tiny droplets, dispersed within another fluid (*Becher*, 1965). The inner phase is traditionally called the dispersed phase, while the outer phase is termed the continuous phase; the two phases usually meet at an orifice.

An emulsion does not form naturally, but it is created by an emulsification process, through which interfaces between fluids are produced and stabilized by some emulsifying agents (*Lissant*, 1974). The breakup of a continuous flow into dispersed droplets is a consequence of the interaction between the viscous stresses, related to the imposed flow field, and the capillary stresses, due to the surface tension between two fluids. The formation of emulsions usually depends on the wetting properties of the employed fluids and on the channel materials: water-in-oil emulsions usually form in channels with hydrophobic surfaces, while stable formation of oil-in-water emulsions generally occurs in channels made of hydrophilic materials (*Dreyfus et al*, 2003).

Considering the double emulsions, they are structured fluids that are formed by emulsion drops with smaller droplets inside. They could be considered as mixed dispersions of more than two immiscible fluids through encapsulation of one layer by the other layer. The double emulsions require the employment of a middle fluid, in order to achieve a complete separation of the inner from the outer continuous phase. Compared to simple emulsions, they are intrinsically harder to create and stabilize, since more phases and interfaces come part of the emulsification process. For the mass production of double emulsions two-step emulsification processes are usually needed; in these processes at first the inner droplets are emulsified in the middle fluid and then the compound is emulsified in the outer continuous-phase fluid (*Goubault et al.*, 2001). Moreover in these processes specific surface treatments are required in order to get hydrophobic and hydrophilic patterns; otherwise a manual assembly of nozzles (or capillary tubes) or complex fabrication methods to achieve the desired 3D structures could be employed. Both the surface treatments and manual assembly processes could imply high manufacturing cost and limited reliability, and so prevent the massive production of these devices. Furthermore, it's difficult to integrate the surface treatment or manual assembly process with the fabrication of common microfluidic systems and therefore the practical application of these approaches is limited.

To produce droplets with a controlled size and at a high frequency, the flow of at least two of the three liquids employed must be controlled by volume, employing a syringe pump, or by

pressure, using hydrostatic reservoirs. The change of the flow rate, in particular the one of the continuous phase, can vary the size of the microdroplets.

Emulsion systems are not in equilibrium, but the use of surfactants can considerably increase their stability. A surfactant suitable for water-in-oil emulsions and another one suitable for oil-in-water emulsions should be dispersed in the middle oil-phase and the outer water-phase fluids, respectively. The employment of surfactants could also change and improve the wettability of the oil-phase and water-phase fluids on the device's wall. In the case of hydrophobic channels for example, it could happen that the middle oil-phase fluid, whose interfacial tension with the walls is much lower than that of the outer water-phase fluid, sticks to the channel surfaces (*Chang et al.*, 2008).

Generally, there are two types of droplet-formation mechanisms: dripping and jetting (*Clanet et al.*, 1999). Dripping produces droplets, which are usually highly monodisperse, close to the exit of the embedded orifice, while jetting produces a long jet that extends into the downstream channel, where it breaks into polydisperse droplets.

The behavior of the flow is well described by the capillary number (1.1), which represents the balance between the drag of the outer fluid, which draws the droplet downstream, and the interfacial tension, which creates a resistance to the fluid movement.

$$Ca = \frac{U\mu}{\gamma}; \tag{1.1}$$

where U is the velocity of the flow, μ is the viscosity of the flow and γ is the surface tension.

Monodisperse droplets are mostly produced by the dripping mechanism and to get a monodispersity as high as possible the downstream channel, close to the exit of the embedded orifice, should be narrowed down to almost three times wider than the orifice is. The reduction of the channel width could increase the fluid flow rates and lateral perturbation around the exit of the orifice, and therefore the dripping break-up would be easier and most likely to occur. Fine control of the fluid flows leads to defined capsule and shell dimensions.

An important issue to be evaluated is the employment of oil or organic phase or mechanical force to generate water-in-oil emulsion (microdroplets), that may damage or contaminate the living cells, and also the exposure of gelled microbeads to oil or organic phase could lead to contamination. Another problem that has still to be overcome in this process is the transport of macromolecules through the interface. For those reasons the pore's size of the encapsulation's material is a critical parameter.

When the double emulsion is created, capsules are then formed by consolidating the middle phase (second fluid) of the resulting double emulsions and this is typically achieved by polymerization of monomers (*Hwang et al.*, 2008) or evaporation-induced jamming of colloidal particles initially added to the middle phase. The crosslinking can be obtained using chemical, thermal or light methods according to the hydrogel properties. The best technique is

photocrosslinking since it allows for a fast and controlled reaction, which can be conducted under ambient or physiological conditions (*Nguyen and West*, 2002). This method involves the conversion of the liquid polymer into a hydrogel through a free radical addition; a photoinitiator is added to the prepolymer to generate radicals after the absorption of ultraviolet (UV) or visible light.

Regarding cell encapsulation there are some worries about the potential cytotoxicity of the photocrosslinking process. However, limitations can be overcome using mild process conditions such as a low light intensity, short irradiation time and low photoinitiator concentrations in the presence of cells (*Nguyen and West*, 2002). Prior to crosslinking, the polymer must often be modified to include two or more reactive groups.

This encapsulation approach has been used to produce monodisperse colloidosomes (*Lee and Weitz*, 2008), hydrogel and ceramic capsules (*Ye et al.*, 2010), and even capsules with composite shells.

1.2.3 Microfluidics for emulsion processes

Microfluidic devices can be used to create controllable droplets emulsions in immiscible fluids, by injecting water (or another hydrophilic compound) into oil (or a hydrophobic compound) through a flow-focusing channel or T-junction geometry (Figure 1.9). Competing stresses drive the interface: surface tension acts to reduce the interfacial area, while viscous stresses act to extend and drag the interface downstream. These stresses destabilize the interface and cause droplets to form.

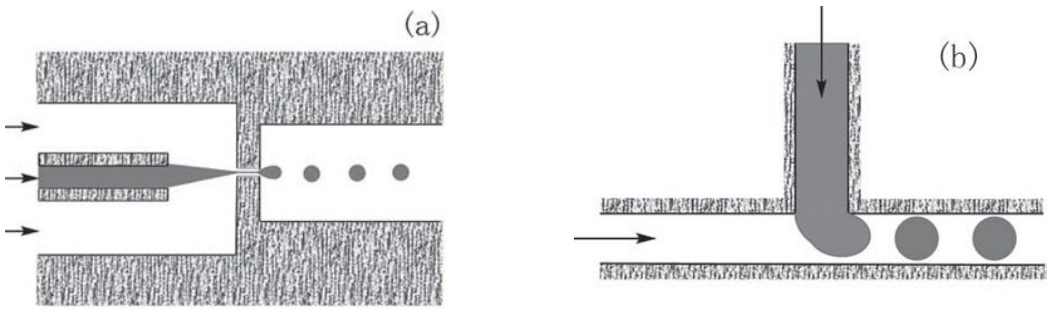

Figura 1.9. *Flow focusing (a) and T-junction (b) geometries.*

In the flow-focusing configuration the dispersed and the continuous phases are forced to pass through a narrow region in the microfluidic device, so that the two immiscible liquid phases undergo large elongational flow when they cross the small orifice and this results in the formation of small droplets. A symmetric shearing by the continuous phase on the dispersed phase enables a well-controlled and stable production of droplets.

In the T-shapes channel configuration the two flows of immiscible liquids are forced to merge so that one liquid forms droplets dispersed in the other. The inlet channel containing the dispersed phase perpendicularly intersects the main channel which contains the continuous phase. At the junction the two phases form an interface, and as fluid flow continues, the top of the dispersed phase gets into the main channel. The shear forces generated by the continuous phase and the subsequent pressure gradient make the tip of the dispersed fluid to elongate into the principal channel, until the neck of the dispersed phase thins and then breaks the stream into a droplet. The dispersed and the continuous phase can be chosen by changing the surface properties, such as hydrophobicity and hydrophilicity, of the device walls at the junction and the relative flow rates of the liquids.
T-junctions present easy fabrication methods, they are also easy to operate and they can be useful if the demand on the homogeneity of the generated droplet size is not too high. With T-junctions high droplet production frequencies can be achieved (up to many hundred droplets per second) and this is influenced by the fluids involved and geometry of the device.
Flow-focusing devices are more complex than T-junction devices and more fluidic inlets are needed; on the other hand flow-focusing geometries allow varying the effective geometry by adjusting the flow rates of dispersed and continuous phase and offer a large flexibility in generated droplets size. By focusing and thinning the stream of the discontinuous phase through an orifice very small droplets can also be generated at high frequencies (*Seemann et al.*, 2012). Flow-focusing configuration seems to be the best choice since it allows better monodispersity and higher frequency of droplet generation than a T-junction; with this geometry a precise control in producing droplets can be achieved.
An important issue when employing microchannels to produce droplets is avoiding contact between the droplets and the device's walls. The first countermeasure is the inhibition of the dispersed phase from wetting the walls of the channels, since if this happens its capillary instability is modified and the process of break-up is difficult to control. The second one is the protection of the new surface of the polymer film, formed in the interfacial polymerization reaction, since if the film is fragile and in contact with the wall, the membrane might be destroyed.

1.3 Materials for microfluidic devices

Today no real standard in terms of materials have been defined, since each microfluidic device has to be designed and fabricated to a specific purpose.
The general requirements for the materials used are the following:

- mechanical properties: both elastomeric and stiff components are needed. Elastomeric properties are useful for valves, pumps and mixers, while stiffer materials for structural support, packaging and interfacing. Microfluidic devices should not be

fragile or brittle because dicing and drilling are often required during the fabrication processes;
- physical properties, such as impermeability, good barrier properties to small molecules, chemical inertness, rapid curing process and high temperature and solvent resistance;
- bonding properties, since bonding between different materials (silicon, glass, polymers, metals) is usually required;
- surface properties, such as adhesiveness, hydrophobicity, biocompatibility, antifouling, surface hardness and roughness.

1.3.1 Glass and silicon

In the past glass and silicon were mostly used for their availability, well developed techniques for fabrication, the potential to merge microfluidics with electronics, their mechanical durability and surface stability. Glass is also suitable for optical detection for its low autofluorescence and his high transparency. These materials are still used in microfluidics, but the processes used for fabricating microfluidic devices from them are too time-consuming and expensive for mass production, so that researchers started to look for new alternatives.

1.3.2 Polymers

Polymers have become attractive for lab-on-a-chip applications for their biocompatibility, low-cost manufacturability, ease of fabrication, rapid prototyping, disposability and wide variety of surface properties.
Furthermore the tendency in the use of polymers as device material finds good reasons after observing that several standard laboratory items, like tubes, pipette tips, polystyrene beads, tubing, cell culture plates, have traditionally been made out of polymers. Therefore the users already know how to deal with these materials and the needed chemistries for their applications have already been developed.
Polymers can be divided in two categories: thermoplastics and thermosets.
A thermoplastic is a polymer which softens at the glass transition temperature (Tg) and can be made to flow when it is heated; it can be processed around a large range of temperature, since Tg and the decomposition temperature (TD) are very different. It hardens on cooling and retains the shape imposed at elevated temperature. This heating and cooling cycle can usually be repeated many times if the polymer is properly compounded with stabilizers. However a certain level of thermal decomposition occurs, so reprocessed material often does not have the same properties as virgin material.

A thermosetting plastic is a polymer that can be caused to undergo a chemical change to produce a cross-linked polymer, called thermoset polymer or resins; they can be either liquid or solid at room temperature. They can often be reshaped to a limited extent with the employment of heat and pressure, but the number of these cycles is severely restricted, since the curing process involves an irreversible chemical reaction. If heated many times the polymer starts its degradation or burns and Tg usually is quite high and close to TD. Thermoplastics such as polymethyl methacrylate (PMMA), polycarbonate (PC), polystyrene (PS) and cyclic olefin copolymer (COC), have become popular material for microfluidic devices for the lower cost of the raw material and fabrication, but many solvents can dissolve them, bonding of device layers is difficult and surface modifications are not easy to realize in many cases.

Thermosets are used in microfluidics for their good dimensional and thermal stability, robustness, permanent surface modifications, chemical resistance and electrical insulation properties. A good solvent can swell a thermoset material but it cannot dissolve it. Compared to thermoplastics, thermosets are more suitable for rapid prototyping since they are shaped either by direct UV freeform lithography or by inexpensive replica molding, without the need of expensive tools and machines.

Nowadays the material used for microfluidic device is usually polydimethylsiloxane (PDMS), which is made by a siloxane chain inorganic and an organic methyl group attached to the chain (Figure 1.10).

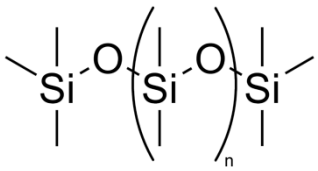

Figura 1.10. *PDMS structure.Figure from Chemfinder.com.*

These polymers have good elastomeric properties, are easy to handle and can be bonded to different surfaces. The polydimethylsiloxane, or PDMS is fluid at room temperature, but can be converted quickly into a solid by cross-linking. In addition PDMS shows a high permeability for oxygen and carbon dioxide and this make it well suited for cell-based systems.

The drawback of the use of PDMS in microfluidics is the difficulty to commercialize it since: higher mechanical resistance is needed; the chemical surface is unsuitable; and scale-up is hard since some steps of the process can't be done on a large scale. Moreover PDMS presents a critical issue for its swelling in common organic solvents and this causes deformation, distortion or even the collapse of the microfluidic channels, so that leaching of uncured monomers and oligomers and leakage from the microfluidic channels may happen. Therefore, it is difficult to conduct many organic reactions or material syntheses with solvents in PDMS-

based microfluidic systems. In order to move from prototype to commercial scale a material with the same mechanical properties of PMMA or PC, but with fast drying and better solvent resistance is needed.

1.3.3 Thiol–ene based polymers

A solution can be the use of thiol-ene for its fast cure, its solvent resistance and low polymerization shrinkage stress, so that thin channels don't change their geometry. Furthermore thiol-ene based polymers present a fast curing with little or no photoinitiator, delayed gel point and not sensitivity to oxygen. These polymers have also many properties in common with PMMA, such as good mechanical properties and solventless formulation.

1.3.3.1 Thiol-ene 'click reactions'

The features of thiol-ene based polymers result from their polymerization mechanism. Thiol-ene based polymer reactions belong to a family called ″click reactions″, which are powerful, very specific, highly reliable, giving high yields of their products and their byproducts can be removed by non-chromatographic methods. Thiol-ene reaction can be consider a ″click″ reaction because it can be carried out under ambient conditions, is fast and it has high selectivity and high efficiency.

The photopolymerization of these polymers is a step-growth radical polymerization, based on the addition of a thiol (–SH) to a monomer with an ene-functional group (carbon double bond). Ideally no homopolymerization occurs. The mechanism of this reaction can be split into four steps (initiation, propagation, chain transfer, termination) and it is represented in Figure 1.11.

a) $$\begin{cases} I \xrightarrow{h\nu} 2I^{\cdot} \\ I^{\cdot} + R - SH \rightarrow HI + R - S^{\cdot} \\ \text{or} \\ I^{\cdot} + R' - CH = CH_2 \rightarrow R' - C^{\cdot}H - CH_2 - I \end{cases}$$

b) $$R - S^{\cdot} + R' - CH = CH_2 \rightarrow R' - C^{\cdot}H - CH_2 - S - R$$

c) $$R' - C^{\cdot}H - CH_2 - S - R + R - SH \rightarrow R' - CH_2 - CH_2 - S - R + R - S^{\cdot}$$

d)
$$\begin{cases} 2R - S^{\cdot} \rightarrow R - S - S - R \\ 2R' - C^{\cdot}H - CH_2 - S - R \rightarrow R' - \underset{\displaystyle |}{CH} - CH_2 - S - R \\ \qquad\qquad\qquad\qquad\qquad\qquad\qquad\qquad R' - \underset{\displaystyle |}{CH} - CH_2 - S - R \\ R - S^{\cdot} + R' - C^{\cdot}H - CH_2 - S - R \rightarrow R' - \underset{\displaystyle |}{CH} - CH_2 - S - R \\ \qquad\qquad\qquad\qquad\qquad\qquad\qquad\qquad\qquad\qquad R - S \end{cases}$$

Figura 1.11 *Mechanism of photopolymerization of thiol-ene polymers: initiation (a), propagation (b), chain transfer (c), termination (d).*

The reaction is normally triggered with a suitable photoinitiator, capable of forming radicals upon UV illumination, but it can be also triggered spontaneously with low wavelength UV-irradiation.

There are many advantages in using UV radiation to initiate the chain reaction: very high polymerization rates (the polymer changes from liquid to solid within a fraction of a second), polymerization only in specific illuminated areas, a lack of inhibition in the presence of oxygen, low shrinkage, good adhesion and high mechanical performance of the UV-cured materials. Moreover this is an environmental friendly technique since no solvents are used and the monomers are not toxic.

During the reaction there is an alternation between propagation, where the thiol radical reacts with the ene functional group, and chain-transfer, which involves the abstraction of a hydrogen radical from the thiol by the carbon-centered radical; this is a key step since it influences the final properties of the polymer. Thanks to the chain transfer the final polymer will have a delayed gelation and a high ultimate conversion, because the trend of radicals to become trapped in the forming polymer network decreases (*Moraga*, 2012). The termination usually occurs by radical-radical coupling.

Since most polymerization reactions reduce the monomer distance, any reactions occurring after the transformation from a liquid to a solid lead to shrinkage stress. Therefore this delayed gelation of thiol–enes greatly reduces the shrinkage stress in the final material, especially compared with other commonly used thermoset materials, such as acrylates, where the gel point is reached early on in the polymerization.

The final network homogeneity has two reasons: firstly, the almost perfectly alternating reaction mechanism between thiols and enes, that are sufficiently electronegative to prevent homopolymerization and to allow a rapid alternating reaction that leads to a polymer structure where crosslinks almost exclusively consist of an equal number of sulfur and carbon bonds. Secondly, the high conversion possible in most thiol–ene polymerizations reduces the presence of regions with a low crosslink density and this is due to the fact that almost all reactive groups are bound into the network. In this way structural irregularities are avoided.

1.3.3.2 Off-Stoichiometry Thiol-Ene (OSTE)

The thiol-ene stoichiometric reaction, described above, has many drawbacks: the finished polymer has non-reactive surface, which requires plasma activation to change the surface properties and no possibility of changing or tuning to softer mechanical properties. For these reasons to achieve a polymer with remaining unreacted functional groups both in the bulk and on the surface the use of the off-stoichiometry in the compositions of the prepolymer has been introduced (*Carlborg et al.*, 2011).

The novel platform consists of multifunctiontal and UV-curable off-stoichiometry thiol-ene (OSTE) polymers, which are specifically developed for microfluidics and lab-on-a-chip applications. These polymers offer direct photo-patternable permanent surface modification, tunable mechanical properties, low permeability to small molecules and solvents and direct dry bonding at low temperature. Other features of microfluidic devices made by OSTE are controlled wetting, hydrophobic stops, capillary filling, pneumatic valves and molding of OSTE fluidic connectors to the chips. The aim of the use of these polymers is achieving a rapid and flexible device-manufacturing platform, in order to bridge the gap between the lab work and high volume industrial production.

The OSTE polymers (Figure 1.12) consist of two types of monomers: thiol functional groups (-SH) and allyl functional groups (-CH_2-CH=CH_2).

(a)

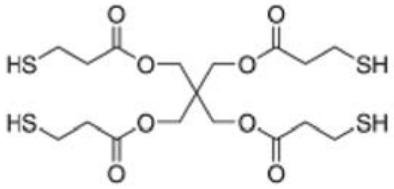

(b)

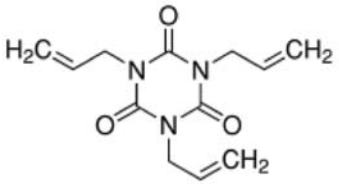

Figura 1.12. *Monomers used for OSTE preparation: tetrathiol(a) and triallyl(b).*

The chemical formulation of OSTE polymers is:

$$xR-(SH)_m + yR-(CH_2-CH=CH_2)_n; \qquad (1.2)$$

where *x* and *y* correspond to the number of moles of each type of monomer and *n* and *m* correspond to the number of functional groups on each.

If $yn = xm$ very few or no groups remain, so that the resulting polymer will have non-reactive surfaces and could require plasma activation to change the surface properties.

If $yn \neq xm$ there is an excess of one of the functional groups and so there is the possibility of achieving polymers with unreacted functional groups, both in bulk and on the surface.

The off-stoichiometry for the thiol-functionality can be described as follows:

$$z(\%) = \frac{xm}{yn} - 1; \tag{1.3}$$

where *z(%)* is the percentage of thiol-functionality excess for the polymer, and *x*, *y*, *m* and *n* are defined as in eq. 1.2.

In order to avoid homopolymerization between monomers with the same functional group and achieve a well-defined amount of unreacted thiols or enes, multifunctional thiol and allyl-ether monomers with well-known step growth polymerization are used.

The density of unreacted functional groups in OSTE polymers can be tuned by changing the off-stoichiometry. The cross-link density presents in the network will in turn affect both the stiffness and the glass transition temperature (T_g) of the material.

The reactive groups left on the surfaces can be used for covalent linking of these to other surfaces, either directly or through grafting with a functional molecule prior to bonding. Bonding is an important part of fabricating microfluidic devices, since they usually require integration of different types of material and assembly of different layers.

Surface modification schemes of the OSTE polymers are simple and occur by exploiting the thiol-ene click-reaction for grafting surface functionalization. Grafting solutions are prepared containing the grafting molecule, a photinitiator and solvents, like water, toluene or isopropanol. The choice of the solvent will depend on the solubility of the grafting molecule. In order to start the reaction the OSTE polymers with the applied grafting solution, is exposed to UV-light. Once the reaction is initiated the grafting molecule will react with the free functional groups on the surface of the polymer.

There are still some requirements not fulfilled by this material: the use of most thiol-ene formulations due to relatively low Tg is problematic, so that the applications of OSTE at elevated temperatures are limited. Other drawbacks are the smell of the thiol monomers and the poor stability of many thiol-ene formulations before polymerization.

However OSTE systems seem to be very suitable for fabrication of microfluidics devices, since the rapid polymerization reaction allows device layer manufacturing times in the order of seconds and the availability of different multifunctional monomers allows a large variety of mechanical and chemical properties, including excellent optical clarity, a narrow glass transition and low permeability to common solvents. Moreover materials and processes to fabricate OSTE devices are very cheap.

1.4 Off-Stoichiometry Thiol-Ene/Epoxy (OSTE(+))

For the fabrication of the microchip a novel ternary monomer system, based on thiol-ene and epoxy monomers has been used. This dual cure polymer material is an extension to the OSTE

family, already described in the previous chapter, and it is called Off-Stoichiometry Thiol-Ene/Epoxy (OSTE(+)) (*Saharil et al.*, 2012).
The addiction of epoxy to the OSTE polymer allows the direct reaction with almost any dry surface and avoids the leaching of uncured components.
Epoxy is a thermoset and it is widely used in the areas of adhesives, coatings, lamination, electronic encapsulation, and composite applications, due to its excellent mechanical properties and adhesive properties. While the thiol-ene networks offers delayed gel points, good control of the polymerization, a uniform cross-linked matrix with high optical clarity, reduced polymerization shrinkage stress, the epoxy networks have good chemical resistance, mechanical strength, excellent adhesion and low shrinkage (*Carioscia et al.*, 2007). For these reasons the development of a thiol-ene/epoxy material can guarantee the formation of a highly crosslinked polymer system, with low shrinkage stress, an increase in the storage modulus, high glass transition temperature and strength.
The main feature of OSTE(+) is its dual cure process; in the first stage the prepolymer is cured with UV-light, resulting in a polymeric material with a soft surface that still has free epoxy and thiol groups, available for bonding and uniform surface modifications. In the second stage, that can be carried out by thermal or UV curing, OSTE(+) changes its mechanical properties, achieving mechanical stiffness and stability, so that it has the chemical inertness needed for microfluidic applications and minimal monomer leaching. The incorporation of epoxy resins into the photo-curable formulation allows the achievement of networks with excellent mechanical and physical properties. Furthermore the epoxy groups introduce into the hybrid networks a greater thermal stability of the cured material.
Using a dual cure process it is possible to incorporate the rigid epoxy structure into the thiol-ene networks achieving great improvements in mechanical and surface properties. The only drawback in some formulations could be poor mechanical and surface hardness properties in the final system, due to the combined effect of flexible thiol-ether linkages during curing, a low crosslink density and a lack of rigid monomer structures.
The monomers used to get OSTE(+) are: a thiol (pentaerythritol tetrakis (2-mercaptoacetate)), an allyl (triallyl-1,3,5-triazine-2,4,6(1H,3H,5H)-trione) and an epoxy (bisphenol A diglycidyl ether), all acquired from Sigma-Aldrich (Figure 1.13). The thiol chosen is mercaptopropionate since it's the most reactive thiol. The initiators used are: photoinitiator Lucirin TPO (2,4,6-Trimethylbenzoyldiphenylphosphine oxide), acquired from BASF, and CGI 1193 radical initiator, from Ciba.

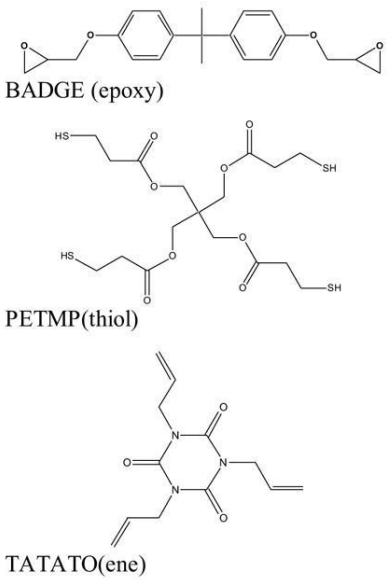

Figure 1.13. *Monomers used for OSTE (+) preparation: bisphenol A diglycidyl ether (BADGE, epoxy), pentaerythritol tetra(3-mercaptopropionate) (PETMP, thiol), and triallyl-1,3,5-triazine-2,4,6-trione (TATATO, ene).*

The off-stoichiometry of the thiol-functionality used for the microchip's material, defined as in eq. 1.3, is 80%, since lower thiol off-stoichiometry would lead to a stiffer material after the first cure, which may obstruct good bonding, and fewer free with fewer free functional groups for surface modification and bonding.

The thiol-epoxy mechanism of polymerization is a catalyzed addition reaction or a nucleophile displacement reaction, and it's represented in Figure 1.14.

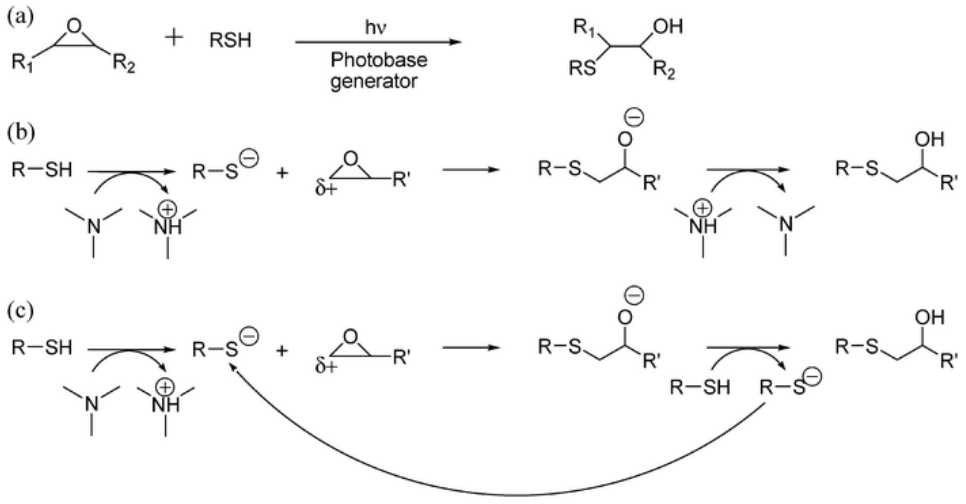

Figure 1.14. *General polymerization mechanism of thiol/epoxy systems.(Figure from Hoyle et al., 2010)*

As can be seen from Figure 1.14, a thiol functional group reacts with a tertiary amine and creates a reactive intermediate, which will result in a thiol anion. This thiol anion attacks an epoxide group via an anionic addition (b) and, at the same time, the tertiary amine can react with the epoxide group creating an epoxide anion.

The most important parameters that influence the reaction mechanism are the initiator and the monomer concentration.

1.4.1 Surface modifications in OSTE (+)

Surface modifications can be conducted on OSTE (+) microfluidic devices.
There are mainly three types of surface modifications: physical deposition of surface-active compounds, direct coupling reactions of polymers onto surfaces (called ″grafting-to″) and grafting of monomers from reactive surfaces(called ″grafting-from″).
The physical deposition of surface compounds leads to noncovalently bound grafts, and this makes the adsorption a reversible process. These grafts may be unstable under high shear forces or other adverse chemical and physical conditions.
The ″grafting-to″ approach employs either Michael addition or photoinduced coupling reactions. The surface modification through coupling reactions has several limitations, comprising incomplete surface coverage, limitations in the diffusion of the polymers into the surface and island formation, due to steric crowding of the reactive sites by the already grafted polymers.
The ″grafting-from″ technique, in which grafts are formed through the reaction of monomers from active surfaces, is an attractive and suitable alternative to form robust grafts and to get great control of the density and functionality of the grafts. In this approach thiol-ene substrates containing initiators or residual thiols are employed to induce the grafting reaction. Each of these approaches involves grafting through radical polymerization, which inherently includes uncontrolled reactions such as termination; for that reason well-controlled grafting in specific zones of a device is usually needed for having an excellent performance.
In OSTE(+) chips reactive groups, such as thiol and epoxy groups, are still present on the surface after the casting process, therefore chemical reactions can be carried out to modify the surface properties. A good strategy to functionalize the surface is the use of the already described ″click chemistry″(par. 1.3.3.1).

1.5 Aim and objectives

This master thesis is the starting point of a project, called TheraCage, followed by Karolinska Institute (Prof. M. Löhr and J. I. Johnsen) and by Polymer MEMS (KTH-Microsystem Technology Lab, Prof. W. van der Wijngaart).
The overall purpose of the TheraCage project is to advance cell-based therapy methods by enabling precisely-controlled polymer encapsulation of therapeutic cells, prior their implantation into a tumor via a blood vessel.

The application focus is to develop a new technology for the treatment of medulloblastoma and neuroblastoma, using transfected cells as a novel drug delivery vehicle, able of subjecting the tumor site to very high doses of a cytostatic drug. Medulloblastoma and neuroblastoma are embryonal tumors of the central and of the peripherical nervous system, respectively. They are the most common and deadly tumors of childhood, where the majority of tumors develop therapy resistance. Refined use of cytostatic drug may improve prognosis, but the accumulated level of systemic delivery of cytostatic drug is close to its limit and many of the survivors suffer great risk of severe consequence from the intensive treatment. For this reason the ability to apply high-concentration of cytostatic drugs directly to cancer cells without affecting normal cells and tissue offers great potential for increasing the effects of cytostatic drugs.

The novel approach will use small size beads, synthetic alternatives to biomaterial, improved core-shell bead morphology and a reproducible microfluidic bead fabrication method.

The specific objectives are mainly two:

- the use of synthetic materials and of a microfluidic fabrication system to provide core-shell beads with transfected cells capable of producing a cytostatic drug in the interior of the bead;
- utilize highly crosslinked porous polymer shell structures for superior dimensional stability and drug permeability, to ensure timely drug delivery to the tumor.

The work of this master thesis will focus on the microchip fabrication, using a novel material platform such as OSTE, and on the controlled production of water in oil microdroplets through an emulsion process. This work will allow the future development of a more complex microfluidic platform, where the double emulsion process to reach core-shell microbeads can be carried out.

.

Chapter 2

Microfabrication methods

This chapter will describe the methods used for the development of the microfluidic platform. It will focus on the microfabrication techniques used for making the microchip, in particular it will describe in details photolithography, PMDS molding process, OSTE (+) mixing, casting and back-end processes.
The general purpose is to show how the processes to make the OSTE (+) microchips can be easily carried out, since they are not time and money consuming.

2.1 Chip microfabrication

The process of fabrication of the micropchip is similar to the commonly used process for PDMS microchip, i.e. soft lithography. The main differences are two: there is no thermal curing, but a faster UV curing and the bonding between the two OSTE layers to get a 3 dimensional channel's structure doesn't require a plasma activation step.
Polymer microfabrication technologies can be divided into two segments: the geometrical structuring of the polymer itself and the subsequent back-end processes. These technologies can also be divided in direct techniques, where each single device is manufactured separately, and replication techniques, where a master structure is replicated into the polymer material. To reach a high throughput in the fabrication of polymer microdevices, fabrication methods based on replication technologies have to be employed.
The steps of the microfabrication process used in this work are mainly five: photolithography, PDMS molding, OSTE (+) mixing, casting processes and back-end processes, which comprise punching, surface modifications and bonding.

2.1.1 Photolithography

Photolithography is an inexpensive and convenient technique which allows for fabrication of microdevices directly, through direct feature patterning, or indirectly, through fabrication of molds, subsequently used to shape polymer materials. The main principle of this technique is the chemical reaction that occurs in a liquid or solid precursor, with photoactive components, when exposed to a specific wavelength of light. The use of a photomask over the precursor blocks the light in specific areas, so that the desired image will be printed on the reactive liquid after the light exposure.

Photolithography results in a patterned master, which is needed in the casting replication method since the required part is molded from the master; this master will contain a negative replica of the part.
The scheme of a standard photolithography process is shown in Figure 2.1.

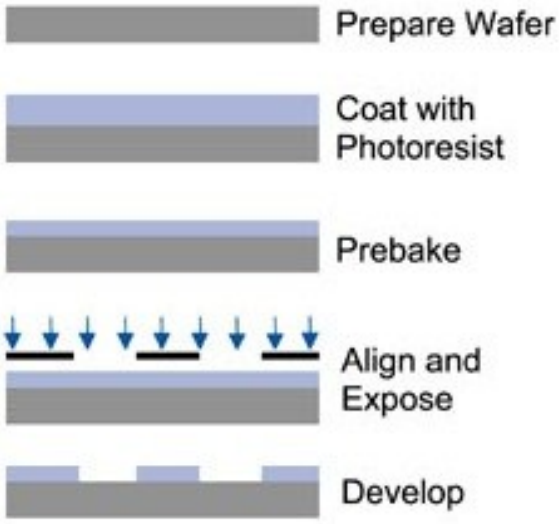

Figure 2.1. *Scheme of a standard photolithography process.*

The starting point for photolithography is the photomask, where there is the desired geometric structure of the microfluidic device. The geometry has to be designed through a graphical software, such as Adobe Illustrator or AutoCAD 2D, and then printed on transparent paper. In this work the design software used has been Adobe Illustrator and to have easier printing and microfabrication processes the following rules have been followed:

- micrometric unit scale;
- at least 2 mm spacing between the borders of adjacent devices, since there will be two chip designed in a silica wafer;
- the minimum aspect ratio, defined as the quotient of the structure height to the minimum lateral dimension (height/width), is 1/10, since structure with lower aspect ratio can collapse;
- the device is designed to function properly despite 30 μm errors in alignment in all directions;

Other parameters, such as surface roughness, flatness of the device or absolute structural height are determined by the master fabrication methods itself.
In this work, the master has been created in a clean room using a silicon wafer and SU-8 2025 (from MicroChem) negative photoresist.
SU-8 is a material designed for micromachining and other microelectronic applications, where a thick, chemically and thermally stable image is desired; its name is due to the fact that its monomer contains eight epoxy groups. The main features of SU-8 are high

mechanical, thermal and chemical stability and the achievement of high aspect ratio in the master. When the photoresist is exposed to UV light a cationic polymerization occurs and a strong crosslinking is reached. On the other hand, SU-8 can be hard to process for its strength, since it generates large internal stresses in the film, which can lead to structural deformations in the substrate. Furthermore, for its good adhesion properties, cured SU-8 is difficult to take off from a substrate, especially from a three-dimensional structure with large surface areas.
The overall process to create the SU-8 master takes less than 2 hours and the main steps are: spin coating, soft baking, exposure, post exposure baking and developing. The times required and the main process variables of each step are represented in Table 2.1.

Table 2.1. *SU-8 master creation: processes times and main features.*

	main process variable	time
spin coating	500 rpm 1150 rpm	10 sec 50 sec
soft baking	67 °C 96°C	4 min 6 min
exposure	365 nm	2 min
post exposure baking	68 °C	7 min
developing	MicroChem SU-8	7 min

Before the use, the silicon wafer is cleaned and dried properly, in order to obtain maximum process reliability.
Spin coating is used to cover certain areas of a substrate with a thin layer of organic material, such as the SU-8 photoresist. The main principle of this microfabrication technique is the centrifugal force applied on the wafer that spreads the liquid resist thinly across the substrate.
A controlled quantity of the SU-8 liquid photoresist is poured into the silicon wafer; during the pouring the photoresist has to be applied in the center of the substrate and it is important to avoid bubbles and not to waste SU-8, since it's very expensive, even more so than the wafer.
After the pouring the substrate is spun according to a defined the schedule, which has been determined looking at the spin speed curve for the SU-8 quality selected. The spin speed curve (Figure 2.2) shows the thickness of the photoresist that can be achieved in function of the spin speed; according to the curve the faster the spin coater turns, the lower is the thickness reached.
In order to get a thickness of 75 μm, the SU-8 was spread out for 10 sec at a speed of 500 rpm and for 50 sec at a velocity of 1150 rpm; the total spin coating time is 60 sec.

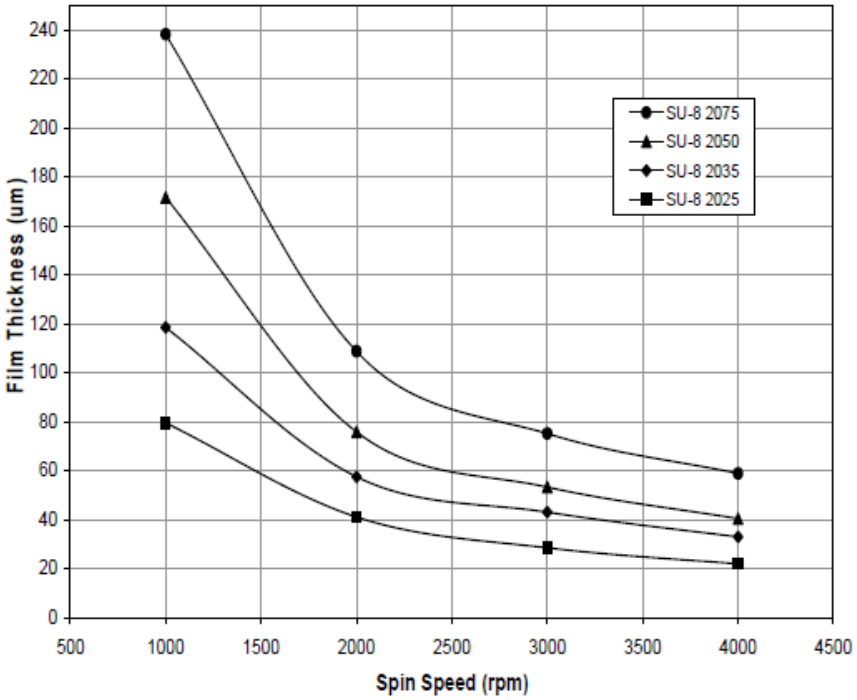

Figure 2.2. *Spin speed curve for different SU-8 photoresist.*

After the spin coating there is a thin layer of soft photoresist on the wafer; during this process step a build-up of photoresist may form on the edge of the layer and, if it's present, this thick bead should be taken off in order to minimize contamination of the hotplate. Moreover thanks to the removal of any edge bead, the photomask can be put in close contact with the wafer during the exposure, so that the resolution of the pattern and the aspect ratio are improved.

The photoresist is then soft baked, using a hot plate, with good thermal control and uniformity, for 4 min at 67°C and for 6 min at 96 °C. To optimize the baking times the wafer is removed from the hotplate after each step and it is cooled to room temperature. The soft baking is needed to relax the mechanical stresses in the material and to evaporate, at least partially, any solvent contained in the resist formulation.

The white field photo mask with the 2-D replica of the desired features, after cleaning with isopropanol, is then used to pattern the photoresist through photolithography. The cross-linking of the resist is achieved in two steps: formation of a strong acid during the exposure step and an acid-catalyzed epoxy cross-linking, activated by high temperature, during the post exposure bake (PEB) step.

To obtain the patterned surface the wafer is exposed to UV light (wavelength of 365 nm). The mask has to be put close to the wafer and then a proper program (in this case ″soft contact″) for the UV exposure is chosen: 6 cycles of 10 sec each, with a waiting time of 10 sec. The exposure is needed to start the SU-8 reaction, so that the desired channel structure will be defined in the resist; after that the photoresist will be still liquid and directly after exposure

the post bake step is needed. The wafer is put for 7 min at 68 °C in a hot plate, the exposed areas will crosslink and form the polymer, while the blocked areas will be still prepolymer, that has to be deleted using chemicals.
The wafer developing consists in dissolution of the unexposed regions in a solvent bath, in order to remove unexposed resist. The wafer is put in the bath with a MicroChem SU-8 developer (Entwickler mr-Dev 600; during the developing strong agitation is recommended to achieve high aspect ratio. When employing SU-8 developer, the developed image must be washed with fresh solution for about 10 seconds, then by a second wash with Isopropyl Alcohol (IPA) for another 10 seconds is recommended. After that the wafer is dipped into water and dried with nitrogen; if there is no nitrogen available it could also be dried with filtered and pressurized air. Through the microscope it is then checked that all the material is polymerized. This chemical wafer's treatment is important to minimize the interaction between the molded part and the master surface, since molding polymers usually undergo shrinkage when cured onto rigid substrates.
To remove minimally cross-linked SU-8 is quite difficult since the photoresist has been designed as a permanent, highly cross-linked epoxy material and it is extremely difficult to remove it with conventional solvent based resist strippers. For that reason a passivation, using TEFLON and a plasma process is needed.
The final real deepness is measured through a profilometer; the results of the SU-8 thickness for the two molds made are: 66 μm and 82 μm.
The SU-8 wafer created has to be stored in closed containers in a cool and dry environment, away from direct sunlight, light, acids, heat and source of ignition; the storage temperature was between 4 and 21°C.
This method has a limited device throughput, since the time needed for preparing the resin and the other process steps is usually of the order of many minutes, so that the total cycle time is too high; for that reason nowadays photolithography is limited mainly to academic use.

2.1.2 PDMS molding

The polydimethylsiloxane (PDMS), already introduced in paragraph 1.3.2, is used to make the mold since it is liquid at room temperature, but it can be relatively quickly converted into solid through cross-linking. The mold is made through a replication method and in its preparation some important issues have to be considered: the geometrical replication result can be as precise as the geometrical accuracy of the SU-8 master, the separation of the mold from master should be easy, no undercuts in the structure itself can be allowed and the surface roughness of the mold should be as low as possible.
The main steps required to make the PDMS mold are:
- preparation of a liquid mixture, containing the prepolymer and a curing agent;

- pouring of the mixture onto the SU-8 master, made through photolithography;
- PDMS's baking and mold extraction.

The PDMS liquid mixture is prepared mixing a base polymer and a curing agent, which is a mixture of a platinum complex and copolymers of methyl hydroxyl siloxane and dimethylsiloxane, both acquired by Dow Corning (Sylgard 184). The two materials are employed in a 10:1 weight ratio; higher or lower ratio can be used to get more or less elastomeric properties in the final structure. The mixture is then mixed vigorously in order to achieve homogeneity. After this the bubbles in the solution have to be driven off, to avoid shortcomings in the final structure; for that purpose the mixture is degassed for half an hour in a low vacuum system.

The elastomeric mold is made through a cast molding process; the mixture prepared is poured into the SU-8 master, on whose surface there is the patterned structure. The pouring occurs in two steps: at first 10.1 g of mixture are poured on the mask and degassed for half an hour, then other 50.5 g of the material is poured.

The master covered by PDMS's prepolymer is put in the oven at 70°C for 2 hours, until the material is completely polymerized. The PDMS's solution becomes a solid and cross-linked elastomer for the reaction that happens between the vinyl (SiCH = CH_2) and the hydrosiloxanic (SiH) groups: the curing proceeds through hydrosilylation, involving the addition reaction between polysiloxane in the base, containing vinyl groups, and the cross-linking agent, containing SiH functional groups. The reaction relies on a platinum catalyst. After the curing process the material has a good chemical and thermal stability, a good gas permeability and low swelling properties. The cured PDMS can be extracted and divided from the master using a scalpel. The mold created is homogeneous, isotropic and transparent, so that it can be put under UV-light without any degradation. The mold's lifetime is generally limited to a few tens to hundreds replications, depending on the complexity of the designs and aspect ratios.

2.1.3 OSTE (+) mixing

OSTE (+) with 80% of thiol excess is the material used for the microchip.

The prepolymer is made through the mixing of three monomers: the thiol PETMP (pentaerythritol tetrakis (2-mercaptoacetate)), the allyl TATATO (triallyl-1,3,5-triazine-2,4,6(1H,3H,5H)-trione) and the epoxy BADGE (bisphenol A diglycidyl ether), all acquired from Sigma-Aldrich. The initiators used are: radical initiator Lucirin TPO (2,4,6-Trimethylbenzoyldiphenylphosphine oxide), acquired from BASF, and CGI 1193 which is a photolatent base from BASF.

All the quantities of the products used are reported in Table 2.2.

Table 2.2. *Calculated amounts of monomers and initiators used for OSTE (+) preparation.*

	off-stoich.	monomer			initiator	
	excess	tetrathiol	triallyl	epoxy	CGI	TPO-L
OSTE (+)	thiol 80%	9.00 g	3.84 g	6.29 g	0.19 g	0.095 g

The quantities of initiators used are: CGI 1 wt/wt % and TPO-L 0.5 wt/wt %.
The mixing steps are the following:
- 1/3 of the allyl used and the CGI initiator are put together in a first bottle, which is then put in the oven at 70°C for 1 hour, to dissolve the solid initiator in the liquid allyl;
- all the thiol, 2/3 of allyl and all the epoxy are put together in a second bottle and then well mixed with a spatula;
- the material in the first bottle is added to second bottle;
- the UV initiator is added to the monomers mixture, which is then well mixed with a spatula and with a mechanical agitator;
- finally 15 min of degasing in a low vacuum system are needed to get rid of the bubbles.
The bottle used has been covered by aluminum foil to avoid early polymerization of the prepolymer.

2.1.4 Casting process

The casting process involves pouring a liquid prepolymer on the replication mold and curing it using heat or UV-light (Figure 2.3).

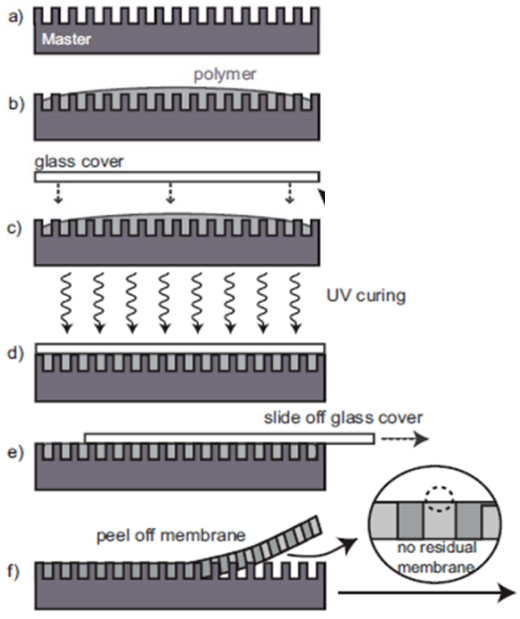

Figure 2.3. *Casting process scheme.*

Casting is an easy process, well suited for small-scale rapid prototyping, since it requires a very small investment in equipment (UV-lamp or oven) and little or no process optimization.
It represents a better solution compared to other plastic mass-fabrication techniques, such as hot embossing and injection molding, since these are designed for a high throughput, requiring expensive machines and lengthy optimization runs (*Sethu and Mastrangelo*, 2003).
In the hot embossing technique the thermoplastic substrate is heated to just above the glass transition temperature (T_g) under vacuum and the it is pressed against a replication master to imprint the microstructures. While during the injection molding the thermoplastic pellets are melted and then injected into a closed replication tool at a high pressure and a high temperature (*Carlborg*, 2011).
The casting technique is able to get high-resolution microfeatures, without the employment of external forces and at low temperatures. In the research field it is the most used microfabrication method to allow the replication of a master pattern, which is the geometrical inverse of the desired structure. Casting is a convenient technique because it requires only few initial equipment costs, mostly for the replication mold, and the prevailing cost is the process time.
However nowadays there are no high volumes commercial casting processes for the replication of micron-sized features and this could limit the capability to scale up production of the prototyped device.
The OSTE (+) prepolymer is cast in the PDMS mold through the following steps:
- the prepolymer is poured into the PDMS mold;
- a glass slide is put over the prepolymer as a filter during UV exposure, while other glass slides are put around the pattern to control the chip's thickness; the glass slide is covered by PDMS to prevent the OSTE(+) from sticking to the glass. The filter is needed to avoid the initiation of the second polymerization, where the epoxy groups react, in the prepolymer.
- the mold covered by the prepolymer is exposed under UV-light (365 nm) to initiate the first curing step, after which the material is still soft and its surface is sticky. The exposure times, found after many tests, are reported in Table 2.3; it has been observed that they depends on the microchip's thickness and the overall exposure time has been split in three steps in order to get a chip with better mechanical properties;

Table 2.3. *UV exposure times for OSTE(+) with 80% thiol excess first curing step.*

thickness	I exposure (sec)	II exposure(sec)	III exposure(sec)	waiting time(sec)
1 mm	80	80	60	20
0.5 mm	40	40	30	20

- the OSTE chip is peeled out from the mold and then cut, using tweezers, a scalpel and scissors.

A flat part is also made using a flat PDMS molds and some glass slides (1 mm of thickness) to control the thickness of the OSTE chip.

2.1.5 Back-end processes

Casting is a planar process, which produces polymer sheets with microstructure only on one side, so the realization of 3D structures requires drilling or punching vertical interconnects between stacked channel layers. In this way the microchannels can be closed. Ports for fluidic access must be opened through the polymer layers to connect to the microfluidic channels; these are called ″chip-to-world connections″, since the holes connect the microscopic structure to the macroscopic world. These processing steps, called back-end processing, have to be carried out to generate the specific functionality. From an economic point of view, the back-end processing steps can reach until the 80% of the device total manufacturing cost.
In OSTE (+) chips the best way to create interconnection is punching mechanically the material, although resolution and spacing between the holes are a constraint. For this chip 1 mm holes are punched. The formation of burrs has to be avoided because it makes a good bonding in the next step impossible or it can close the microfluidic channel branching off the hole.
The channels walls must be functionalized in order to get PEG microbeads in oil; for that purpose the channels has to be hydrophobic.
The patterned part with holes and a flat part are put together, one above the other, and the OSTE microchip is surface modified by dripping modifying solution into their channels with a syringe and placing a transparent masking film on top. This film is used to avoid evaporation of the modifying solution from the surface of the chips.
The hydrophobic homopolymerizable modifying solution is prepared by mixing 5 wt % of liquid heptadecafluorododecyl methacrylate, 1 wt % of Lucirin TPO initiator and 1 wt % of initiator benzophenone (Aldrich), used as received, in 5.0 g of toluene. The modified microchip with the solution in its channels is exposed for 5 minutes to UV-light. The introduction of fluorinated components to the modifying solution confers to the sample the hydrophobicity required. Completely hydrophobic surfaces can be obtained with mixtures with very low amounts of this compound. Then a toluene rinsing solution is utilized to wash the channels and clean them from the modifying solution; after that the chip is well dried with nitrogen.
This method allows to functionalize the channels surface and to bond the two OSTE layers at the same time, using the free thiol and epoxy groups. When the microchip is under UV light the second polymerization happens and no free groups are left in the channels surface.

Chapter 3

Microsystem's characterization

In order to have an efficient fabrication of the microfluidic device whose application will be a drug delivery system, some characterization tests are needed; these tests will help to fine tune the system.
This chapter will deal with the following characterization's methods: the contact angle measurement, which assesses the hydrophobicity of the patterned part of the microchip after the surface modifications, the flow test to verify that there is no clogging in the channels, and finally the bonding test to check the presence of leakage and the quality of the adhesion strength between the two layers of OSTE (+) material, which form the microdevice.

3.1 Contact angle measurement

To verify the hydrophobic properties of the microfluidic device the contact angle measurement, which is a technique of characterization of the surface wettability, has been employed. This method can confirm the efficiency of the surface modifications in the microfluidic channels.

3.1.1 Principle

The contact angle between a solid surface and a liquid droplet is a measure of the ability of a liquid to wet the surface and it is related to the free surface energy of the solid material: in fact from this measurement the surface energy of the material can be calculated. The calculation of the contact angle allows knowledge of the affinity of a liquid, such as water, to the solid surface of a microchip. Using water as a test liquid it's easy to see if the surface is hydrophobic (formation of a great angle, > 90°) or hydrophilic (formation of a small angle, <90°).
The contact angle in microfluidic channels is also the boundary condition that defines the shape of the liquid/liquid interface (*Cubaud et al.*, 2005).
If the energy required to create the solid-liquid (γ_{sl}) interface is higher than that required for formation of a solid-gas (γ_{sg}) interface, the critical angle will be greater than 90° and the surface is considered hydrophobic. The liquid will not spread on the surface, but it will form

spheres to minimize the solid-liquid interfacial area; the relation between the contact angle and the surface tensions is given by the Young's equation:

$$\gamma_{sg} = \gamma_{sl} + \gamma_{\mathrm{lg}} \cos\theta ; \tag{3.1}$$

where γ is the surface tension, which can be defined as the energy required to create a unit area of an interface, γ_{sl} is the surface tension between the solid and the liquid, γ_{sg}, and γ_{lg} are the surface tension of the solid and of the liquid, in equilibrium with their saturated vapor, respectively. This equation is the result of the mechanical equilibrium at the contact point between the liquid droplet and the solid surface.

The Young's equation describes the thermodynamical equilibrium of the system, which is very hard to realize experimentally, since that condition of lowest free surface energy is reached only if the surface is stiff, still, smooth, homogeneous and it doesn't interact with the liquid. At the equilibrium point the system has only one contact angle. For those reasons, when calculating the contact angle, it's important to consider the measurement method and the operative conditions employed. This information is needed also for the experimental repeatability.

Two different type of contact angles can be measure: static angle and dynamic angle. The static contact angle is determined by the interfacial tensions and it's formed when the liquid deposed is not in movement. The dynamic contact angle is determined by the equilibrium of interfacial forces and viscous forces and it's formed in presence of liquid flow.

In the tests carried out static contact angles have been measured.

The method utilized consists in calculating the angle between the outline tangent of a drop deposited on a planar solid surface, which is the microchip's surface, and the surface of this solid (Figure 3.1). The contact angle is measured at the contact location.

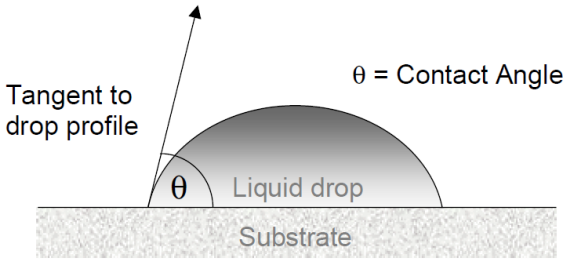

Figure 3.1. *Contact angle measurement method.*

The assumptions made for the measurement are:

- the droplet is symmetric about a central vertical axis, so it doesn't matter the direction from which the drop is viewed;

-the gravity force doesn't influence the shape of the drop and it's neglected;

-the patterned surface is homogenous and smooth.

This goniometric technique is convenient and very easy to perform, since the contact angle is calculated through direct inspection, but there could be large inaccuracies and variance in the

contact angle measurements, due to a not proper user interpretation of the tangent line and surface, improper imaging and poor images (*Woodward*, 1999).
Moreover there are some factors that can influence the contact angle measurement and these are the surface preparation and its chemical composition, contamination factors, the external environment, the temperature and the droplet dimensions (*Woodward*, 1999).
If the surface is heterogeneous, for contamination or for roughness, the contact angle can vary, while the environment's action is due to vapor absorption of water in the polymer surface, and this could reduce the superficial tension. Furthermore contact angles can increase or reduce with the change of the temperature, but the variation is significant only near the boiling point of the testing fluid, where it shows a reduction of the interfacial tension and the contact angle tend quickly to zero.

3.1.2 Testing

To test hydrophobicity water is needed as test fluid; moreover it's safe and it should form a high and easily observed contact angle. Diluted food dye can also be used since it's mainly composed by water and it makes easier to see the profile of the drop.
A drop is deposed on the patterned surface using a microsyringe and a needle of 20 gauge, 0.025"id x 0.036"od (from CML Supply). The droplets deposited have a diameter of about 1 cm, which is 5 times the channels height.
A profile image of a drop taken with a camera, like the one shown in Figure 3.2, has been used to measure the contact angle.

Figure 3.2. *Droplet's profile upon unmodified OSTE(+) 80% material.*

The camera is placed to look exactly horizontally at the drop when the picture of the system, formed by the solid sample and the drop, is taken; the camera angle does not affect the reading but it does profoundly affect finding the baseline, which influences the reading.
The pictures acquired are processed by a computer and the contact angles are calculated using the imaging software ImageJ and its contact angle tool. After tracing the line of the planar surface and the tangent line to the droplet, the software is able to evaluate the contact angle.
To assess the surface modifications efficiency a measure of the contact angle of unmodified OSTE (+) 80% microchip has been carried out before the test. Four different droplets have

been measured and the contact angle was 71°, which results from the average of measured number of measurements. Since it is lower than 90° the surface of OSTE(+) 80% is in the hydrophilic domain.

Afterwards the contact angles of 16 different droplets on the modified patterned surface have been calculated.

In Figure 3.3 the values of the different contact angles measured are represented.

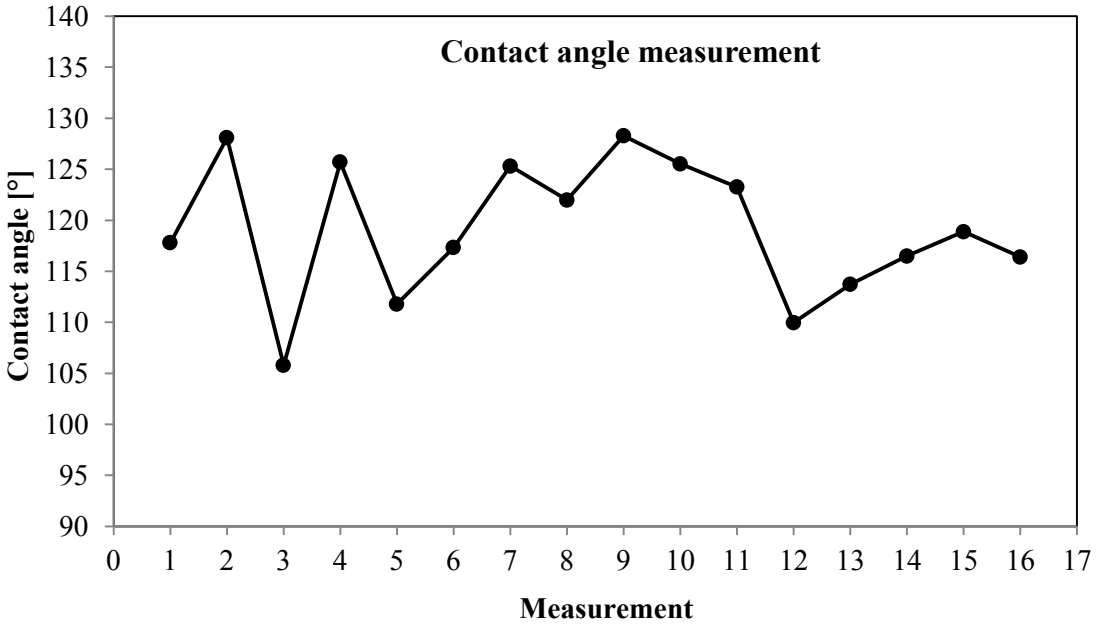

Figure 3.3. *Contact angle measurements.*

The contact angle achieved results from the average value of the sixteen measurements performed in different points of the pattern and in different devices. The resulted value corresponds to 119° ±7°, so the surface can be definitely considered hydrophobic and suited to formation of water in oil droplets.

Other information about the contact angles measured are reported in Table 3.1.

Table 3.1. *Contact angles measurements statistic data.*

statistic data	angle
min	105°
max	128°
mean	119°
std	6°
range	22°

The statistic data confirm the hydrophobicity of the channels walls, since all the contact angles measured are higher than 90° (min. value = 105 ±7°).
It must be considered that the contact angles measured are not the real contact angles at the equilibrium point, but they are measured in a metastable condition, so the real values could be either lower or higher than the ones measured. However, since the calculated angles are much higher than 90°, the patterned modified surface can be defined hydrophobic and it satisfies the requirement for the microchip's application desired.

3.2 Flow test

The flow test is a preliminary characterization test which helps to understand the sealing properties of the microfluidic device fabricated through the evaluation of the leakage in the system (*Goh et al.*, 2009).
The test consists in putting a droplet of distilled water containing green food dye at one end of a channel of the bonded chip and placing a vacuum suction tube at the other three ends. The color dye will fill up all the channels if there is no blockage in the device.
A sample size of six devices has been used for the test and they have been observed at the microscope for 5 minutes.
The results show that the fluid is able to flow freely in the channel and no channel blockage has been detected, as it can be seen in Figure 3.4, where a bonded chip that has passed the flow test is represented.

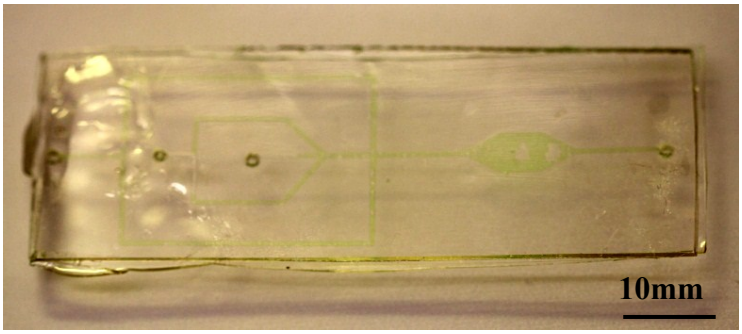

Figure 3.4. *Colored pattern for the fluid test in the microfluidic device.*

Since after 5 minutes, a testing time suggested by other works (*Goh et al.*, 2009), the liquid has remained in the channels, it is demonstrated that there is no leakage in the system and good sealing properties are verified.

3.3 Bonding test

Full-wafer bonding is a fundamental technology for the fabrication of microfluidic devices and characterization of the bond has become an important issue to fulfill the high-reliability demands, particularly for medical applications (*Rabold et al*., 2009), such as the one of the microchip developed in this project. The bond strength is an important factor to guarantee a reliable lifetime of a microfluidic device, and it is considered one of the most important features to be determined (*Rabold et al*., 2009).

Since the two OSTE (+) layers are covalently bonded together after the second cure, they are prone to brittle fracture due to their strong and directional atomic bonds. These materials have no capacity for macroscopic permanent deformation and cannot redistribute stress by plastic flow. The size of the stresses applied and the size, the shape and the distribution of internal flaws govern the fracture's behavior. Small structures in the cured material, such air bubbles, are the points where the crack can start.

The adhesion forces between the two polymer layers must be sufficient to sustain normal pressures, i.e. 1–2 bars, typically encountered in microfluidic LOC applications (*Saharil et al.*, 2012).

The bonding test will quantify the adhesion between two OSTE (+) 80% bonded layers, the patterned one and the flat one, used to form the microfluidic device. If a fracture occurs, the fracture pressure will be recorded and this measure can give an estimation of the adhesive strength. The purpose of this test is to evaluate the maximum pressure that the bonded microchips can withstand.

The most common methods for bond-strength measurement are the double cantilever beam test, the tensile test, the chevron test and the blister test. The double cantilever beam test can be used with unseparated wafers, but it uses large areas for characterization, while the other tests have to separate the wafer in samples, so they are therefore unsuitable for an on-wafer characterization: in fact they are destructive tests (*Vallin et al.*, 2005).

To ensure adequate bond performance and to test the quality of the microfabrication method, the pressure tests have been carried out using six samples of the microfluidic device.

For each device analyzed, all the inlet or outlet ports have been closed with tape, except for one inlet, where the pressure is applied using a pressurized nitrogen gas tank, equipped with a pressure regulator. The regulated nitrogen supply and pressure transducer are connected to the devices. In this way the static pressure applied to the device can be controlled and monitored. The applied pressure is first set at 1 bar for 2 minutes.

If there is a drop in the pressure gauge or bubbles are formed in the bonded chip or a crack propagates through the bond interface, which means that the microchip has failed the test due to pressure leakage at the pressure set, which will be the critical pressure that leads to failure of the bond interface. If no leakage occurs after 2 minutes, the pressure is increased in steps of

1 bar and held for 2 minutes at each interval pressure. In this way the pressure is slowly increased until gas leaked out or the pressure limit (5 bars) of the set-up is reached.
This test is easier to carry out than the well-known blister test, where a load is applied to the bond interface by pressurizing internal cavities sealed through wafer bonding; the pressure required to start the fracture at the bond is estimated as the bond strength. The main difference between the two tests is that the crack is generated internally only, while the blister test destroys the upper wafer by blowing out the upper membrane (*Vallin et al.*, 2005).
The pressure test conducted show that there is no sign of delamination or gaps formation in the bonded chip for all the chips tested. A test fluid pressure of 5 bar has been reached; this value can be considered relatively high and gives a good indication of the reliability of the bonded microfluidic chip under pressurized liquid flow, since the channels were able to withstand that pressure without chip interface failure. For that reason the device fabricated has succeeded also the bonding test.

Chapter 4

Microsystem's development

In this chapter the development of the microfluidic platform is described.
At first the geometrical structure of the microdevice is presented.
In the second paragraph it's shown how to connect the microsystem proposed with the macro world, through the commonly defined ″one-world-to-chip″ connections.
The third paragraph is about the setup needed for the experiments, and the experimental results are discussed in the last part of the chapter. Both water in oil and oil in water emulsions are evaluated, in particular the effects of the flow rate ratio on the size and on the frequency of droplets production are analyzed. Moreover the different regimes of flow of the two immiscible liquids in the microchannels are examined.

4.1 Proposed design concept

The goal in this drug delivery microdevice is to generate the droplets as small as possible because larger droplets are less stable and more likely to come in contact with each other, and this causes droplet deformation and coalescence. Moreover other studies have determined that 50-150 μm droplets ensure an optimal size for cells used in for drug delivery applications (*Adzima and Velankar*, 2006.). It's also important to get an active and precise control of the size and of the production frequency of the droplets.
Considering these desired properties, a flow focusing configuration has been chosen for the device; this effective geometry will be able to form tunable microdroplets by changing the flow rate of the two fluids, as already described in the first chapter (1.2.2). Discrete liquid droplets will be encapsulated by a carrier fluid that wets the channel surface and forms the continuous phase, while the droplets will be isolated and will form the dispersed phase.
In the development and fabrication of flow focusing microfluidic devices numerous dimensions in their geometry have to be considered, since they might play an important role in the droplet breakup process.
The main geometric dimensions, on which the emulsion process depends are the following:
- the depth of the channels h;
- the width of the upstream channels for the continuous phase liquid;
- the width of the upstream channel for the dispersed phase liquid;
- the width of the downstream channel;

- the junction's angle ϕ.

The model geometry developed (Figure 4.1) consists of two junctions: one for the formation of the oil in water emulsion and one for the formation of the water in oil emulsion.

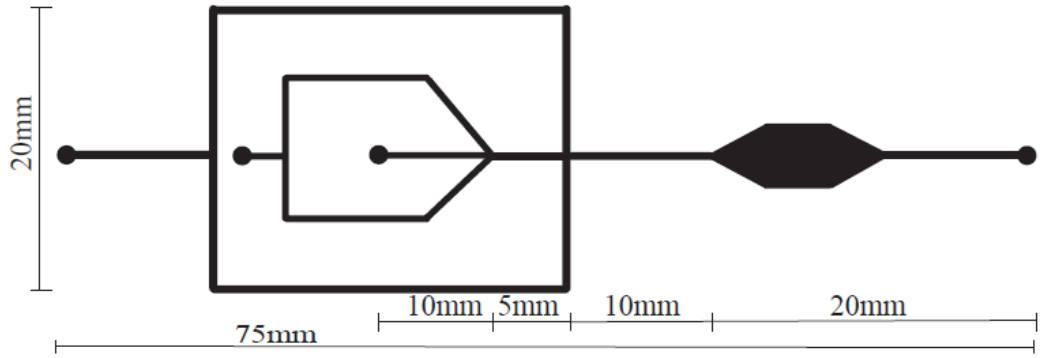

Figure 4.1. *Schematic microchannel geometry for hydrodynamic flow focusing.*

The two junctions have different contact angles, in order to investigate simultaneously how the junction's geometry influences the droplets breakup process and the influence of hydrophobicity on droplet formation. The first two side channels form a 45° junction with the longer channel, while in the second junction the side channels form a 90° angle. The whole device is 75 mm long; where the 50 mm long channel form the first junction 7.5 mm from the inlet end of the inner phase, while the second junction 15 mm from the same inlet end. All channels are 200 μm wide and 75 μm deep. There is one inlet for each phase and one multiphase outlet; a collector of the droplets formed has been designed along the main channel, 10 mm from the outlet end.

Considering the design proposed for the microfluidic system the following considerations should be done in order to provide a description of the fluidodynamic behavior inside the microchannels:

- since the system dimensions are reduced, fluids are increasingly influenced by viscosity rather than inertia and this results in laminar flow (Re <<1), which is more controllable and predictable;
- high surface area-to-volume ratios ensure that surface tension influences fluid behavior;
- since mass and energy are transferred quickly, the system can be considered homogenous and isothermal;
- the mass transport occurs without dispersion and it is controlled by flows velocities and system dimensions.

The volumetric flow rates of the continuous phase (Q_c) and of the dispersed phase (Q_d), are controlled independently and each influences the process differently. By varying the amounts of input reagents the droplets can be dosed and also generated at high frequencies. The droplets size will be well-defined since the geometry chosen allows getting a monodispersed flow of droplets.

4.2 One-chip-to-world connections

″World-to-chip″ interconnections, also called macro-to-micro interface, allow the coupling of on-chip microchannels to macroscale off-chip devices, such as a syringe pump. Currently, the connection of a microfluidic device to the outside is still a big issue to be solved and it's one of the reasons that prevents the process automation, large scale production and so the commercialization of microfluidic devices (*Fredrickson and Fan*, 2004). This is one of the greatest restraints for the acceptance and the application of μTAS into the broad world market (*Kortmann et al.*, 2009). For the success of these devices this issue has to be overcome and good ″world-to-chip″ interconnections must be developed, in particular for high-throughput applications, where manual manipulation is not economical (*Westwood et al.*, 2008). The overall process to make the chip and these connections should be convenient, reliable, flexible, durable and fully automated. If these features were reached, the microfluidic device would find a successful market, since there is a high industry demand for simple and rapid chip interfaces.

The main problem in realizing this kind of connections is due to the fact that collected samples and reagents have to be transferred in quantities of microliters to milliliters (or even liters), whereas microfluidic devices require only small volumes of reagents or samples, in the order of size of nanoliters or picoliters, since the dimensions of the channels are on the order of microns. Moreover handling micro-scale flows and using microfluidic devices of different kinds with different demands on connections make the development of chip-to-world fluidic interconnects one of the major challenge in microfluidic systems fabrication (*Fredrickson and Fan*, 2004). The interconnect schemes commonly used are expensive, require additional fabrication efforts and are highly prone to failure, leaking and clogging.

The features that should be addressed in the production of an ideal micro-to-macro interface are the following:

- ease of assembly;
- reliability, which means no leakage at standard operating conditions for the desired application;
- chemical compatibility, since materials used in the assembly should not influence or react with the samples;
- minimal dead volume; there shouldn't be areas where fluid does not circulate because these dead volumes increase reagent usage and reduce precision and efficiency;
- maximum field of view, in order to collect data when the analysis will be conducted optically, such as by a microscopy;
- ability to operate over a large range of flow rates;
- low cost and user-friendly;
- full automation;

- minimal pressure drop when the flow is pneumatically driven; pressure drops are usually caused by the geometry of the system or by a constriction;
- not requirement of skilled personnel, multiple manual steps, and special devices;
- process to make them not time consuming and that damage the chip;
-high mechanical strength and low leakage.

Actually there is no single approach that fulfills all the requirements, but some of the criteria must be fulfilled according to the specific application, so a good interface will exist for each different device (*Korivi and Jiang*, 2007).

There are several products available and techniques that have been used to provide interfacing between microchannels to external device, such as syringe pumps. The most commonly used approach is connecting tubing between each other's and directly to the microchip by the insertion of the tubing into a punched inlet and by use of glue, such as a cured epoxy. The drawbacks of this method are that the tube attachment will be permanent, channel clogging could occur due to the glue used, the tubing employed, usually made of plastic, may not adhere well to epoxy and so they need additional assembly time and there might be leakage of liquid from the connections, especially when high pressure inlet are required. Furthermore there could be a high cost of the commercial devices. The advantages in these interconnections are that these types of interconnections can be removed and eventually reused.

The problems that should be considered in finding a good solution for interconnections are:

- adhering and aligning the tubing to an edge; since most devices are not planar also after a controlled microfabrication, this step is rather hard and isn't always a failure-proof method of creating a connection;
- having the dimensions of the interface agreeing with the existing industrial standards for the desired application; since the dimensions and tolerances of the device are small, (distance between ports in some devices is less than a millimeter), there could be dimensional incompatibilities;
-the properties of the materials for interconnects must be compatible to the device's material;
-stability problems created in the micro-scale device by physical stresses, caused by the macro-scale fluidic connector;
- leakages of fluid in the system, due to failure or inability to handle the fluidic pressures by the fluidic interconnect components and to the use of a non-uniform clamping force to ensure proper sealing between various layers of the device.

OSTE (+) microchips overcome the main problems in interconnections of the commonly used PDMS microchips, where disturbance to the needle may damage the material around it and produce small cracks leading to leakage around the needle. Moreover the connections can fail at low pressures for the weak adhesion of the glue typically used to PDMS. The insertion of the tubing directly into the inlet may also affect the flow if the tubing is pushed right to the

bottom of the channel, and thereby increasing hydrodynamic resistance, in particular if the microchip is made from a thin layer of PDMS. After these consideration PDMS doesn't seem to offer many advantages in the fabrication of connections; however it has to be considered that OSTE(+) 80% is a quite new material for microfluidic devices and so a lot of matters have to be treated in its usage.
The development of the fluidic interconnects has been considered in order to fit the features of the material and it's based on the achievement of a leakage-proof operation, with high reliability and ease of handling, but without long time requirements in making the setup.
In Figure 4.2 the components used to make the micro-to-macro connections are represented.

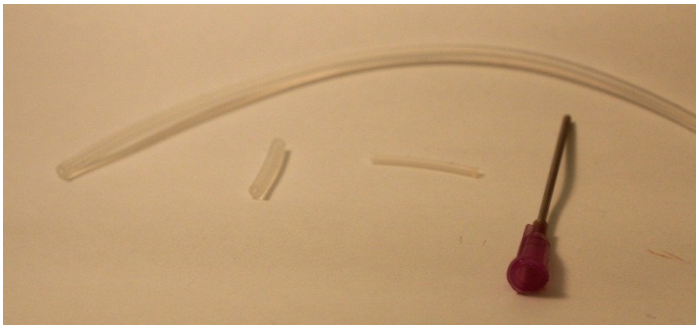

Figure 4.2. *Parts used to make a world-to-chip connection for an OSTE(+) microchip.*

The parts used, described in detail, are the following:
- two silicon tubing, a long one and a short one, 1/16″id (from Buch & Holm, Denmark);
- ETFE (poly(ethylene-co-tetrafluoroethylene)) tubing, 1/16″od x 0.05″id (from VICI AB International, Switzerland);
- a needle, 16 gauge, 0.053″id x 0.065″od, ½″ blunt tip stainless steel canula, overall length 1.690″, UV safe plastic tube with luer taper (from CML Supply, Lexington, USA).
A double quick epoxy glue from Biltema (Sweden) is also used.
The steps for the fabrication of the interconnections are the following:
- plugging the ETFE tubing into the silicon tube (Figure 4.3);

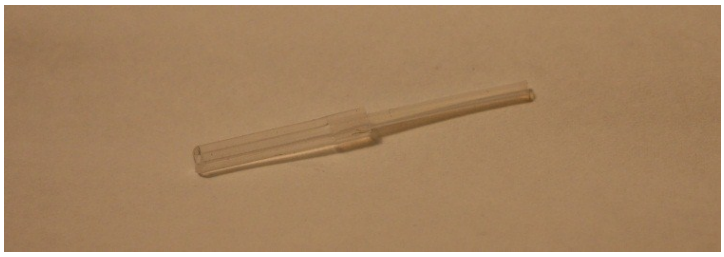

Figure 4.3. *ETFE tubing inserted in the silicon tube.*

- plugging the ETFE tubing into a long silicon tube (Figure 4.4), which will be later connected to the syringe pump, through the needle chosen;

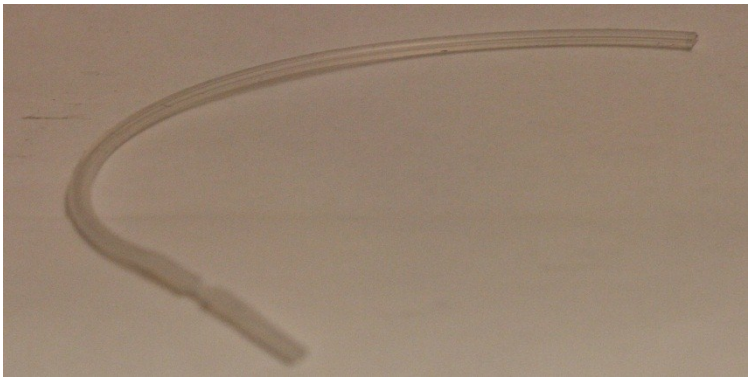

Figure 4.4. *Connection between different ETFE and silicon tubes.*

- fixing the smaller silicon tube to the microchip through the use of a double epoxy glue; a tube is aligned and adhered to each inlets and then surrounded by the glue. The glue takes 15 minutes to cure; after that the connection's system is well glued to the chip (Figure 4.5).

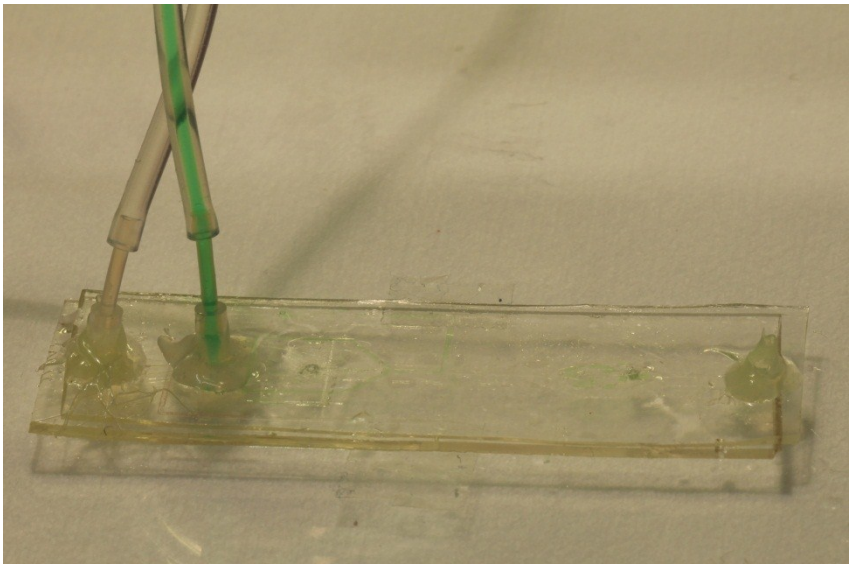

Figure 4.5. *World-to-chip connection for an OSTE(+) microchip.*

In all these steps it's very important to position the tubing properly, in order to avoid leakage problems and clogging problems, due to the uncured glue, and to get a leak tight system.
The technique described is very simple, inexpensive and robust, it allows a setup for the usage of the microfluidic device easy to build and that can be realized in less than 30 minutes. Moreover the interconnection system developed is characterized by optical transparency, and this is important since it is necessary to visually monitor in real-time the emulsion processes occurring in the device.
After designing and fabricating these interconnects, they have been tested to see if they fulfill the needed requirements. Leakage has been tested by filling the channels and then using a

pump to pressurize it until failure is observed. Mechanical strength has also to be tested by pulling the capillary tube until failure occurs.
The tests have been done using water as a fluid to fill the channels and it has been shown that no leakage occurs.
Another good solution for interconnections, also in order to reduce the fabrication steps, could have been the creation of interconnections during the initial molding process and modifying the design of the microfluidic device, in order to incorporate the desired characteristics (*Carlborg et al.*, 2011).

4.3 Experimental setup

The fluids used for testing the emulsion process are light mineral oil (from Sigma-Aldrich, USA) and distilled water. The physical properties of the two fluids are reported in Table 4.1.

Table 4.1. *Physical properties of the fluids used for the emulsion process.*

Physical property	**Value**	**Unit**
distilled water density	998	kg/m^3
water viscosity	0.001	Pa*s
mineral oil density	838	kg/m^3
light mineral oil viscosity	0.075	Pa*s
surface tension	50	mN/m

All the properties reported in Table 4.1 refer to room temperature (25°C) and it is assumed that they all remain constants at their established values at this temperature. The surface tension reported is an estimated value, found from published data for light mineral oil and water systems with 2% of surfactant Tween 20 (*Shelley*, 2009). Technical Tween 20 (polyoxyethylene (20) sorbitan monolaurateornitore, from VWR International, Prolabo BDH, France) is added to the distilled water as a surfactant. This surfactant (Figure 4.6) is a polysorbate surfactant and it has been chosen for its stability and relative non-toxicity.

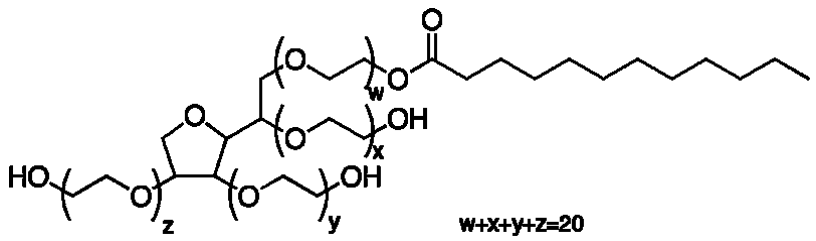

Figure 4.6. *Chemical structure of the surfactant Tween 20 (figure from Chemfinder.com).*

Some food dye is added to the distilled water solution to monitor more easily the droplets formations through the microscope; the food dye will not change the properties of the fluids, since it mainly consists of water.
In order to study and to get a first stable continuous process of droplets formation in the microfluidic device water is used instead of PEG, which will be necessary for cell encapsulation. Some trials with PEG have also been conducted, but the proper quantity of PEG dissolved in water have not been set yet, since high PEG concentrations (50-60 %) increase the viscosity to a large extent and the interaction with oil is completely different compared to the one with the water.
In the experiments carried out the dispersed phase is always surrounded by the continuous phase and has fewer tendencies to wet the walls of the channels than the continuous phase, since the walls are hydrophobically modified. The flow rates of the continuous phase have been initially set higher than the flow rates of the dispersed phase, until the creation of a conic tip is reached.
The variable which controls the droplets size is the ratio between the flow rates of the outer and of the inner phase.
The fluids are driven by programmable syringe pumps (model 540060, from TSE systems, USA), shown in Figure 4.7.

Figure 4.7. *Programmable syringe pump(model 540060, from TSE systems, USA).*

Disposable syringe NORM-JECT 5mL volume in luer (from Henke-Sass, Wolf GmbH, Netherlands) are used and they are connected to the tubing through a dispensing tip with the following features: 16 gauge, 0.053″id x 0.065″od, ½″ blunt tip stainless steel canula, overall length 1.190″, UV safe plastic tube with luer taper (from CML Supply, Lexington, USA).
The syringe pumps deliver the continuous-phase and the dispersed-phase liquids into the flow focusing channels and they maintain a specified volume flow rate by appropriate adjustment of the force applied to the syringe, which changes the pressure in the fluid. In a multiphase

flow the shape of the fluid-fluid interface is determined by the flow itself. The syringes are connected to their respective inputs of either the dispersed or the continuous phase channel. The syringe approach for fluid delivery requires the choice of a tube diameter and then uses standard motor-driven pumping to achieve a given flow rate. For the diameter a value of 10 mm is set; this value is equal to value of the diameter of the syringes used.
The flow rates for each fluid have been maintained between 100 μL/min and 1 μL/min, that correspond to Reynolds number, defined in equation 4.1, $Re_{min} = 0.12$ and $Re_{max} = 11.86$:

$$\mathrm{Re} = \frac{\rho v d}{\mu}; \tag{4.1}$$

where ρ, v and μ are the density, the speed and the viscosity of the continuous phase, respectively, while d is the width of the channels.
The process of forming and manipulating the droplets were observed using an optical microscope (from Leica Microsystems AB, Sweden); the images and the movies has been recorded using an imaging software that integrates Leica automated microscopes, called Leica Application Suite. This software allows for real-time and high resolution imaging. Other images and movies have been taken using a digital camera (Canon, model EOS 650D).

4.4 Experimental analysis

The overall objective of all the experiments performed is the achievement of a uniform, regular and constant droplet formation, characterized by a high frequency of formation of droplets, with a droplets diameter comparable to the channel's width. The emulsion processes were carried out in the microfluidic platform described previously.

4.4.1 Quantitative measurements

To understand the influence of the flow rates of the two monophasic fluids on the droplets formation, in each experiment the following parameters have been calculated: the distance between two consecutive drops, the drop length, which is a measure of the drop size, the velocity of the droplet in the channels and the production frequency of the droplets.
In each experiment drops of a certain size are formed at a given frequency f and move down the channel at a speed u.
Measurements are taken with a digital camera (Canon, model EOS 650D) and analysis of the movies recorded and of the pictures taken are performed using an image analysis software to first find the drop size and position in each movie frame and then stitch positions together to produce complete tracks for each droplet. From the evolution of drop's position and size with time all the relevant parameters are calculated.

The velocity of the droplets, u, is measured by using the numerical derivative of its position with respect to time, by tracking the drop center of mass for a short distance down the channel. The frequency of production f is calculated from the time delay between successive droplets to pass a fixed reference point in the channel, by direct counting from the video.
Previous studies tells that the distance between two consecutive droplets (d) should be sufficiently large compared to the channel width to get a stable train of droplets. The speed of the drops (u) expected is closed to the average velocity of the continuous phase.
The quantities d, u and f have been measured independently and, on geometric grounds, the equation $fd = u$ is expected to be satisfied.
Both water in oil emulsions and oil in water emulsions have been performed; for the w/o two different junction's geometries (90° and 45°) have been evaluated.
In all the experiments carried out the continuous phase flow parameter is held constant, while the dispersed phase flow is decreased until, from the liquid jet, droplets formation occurs.
At first the start-up behavior of an initially droplet-free channel has been measured by raising the liquid velocity above the rate at which the liquid thread retreats from the outlet; then, once the device is cleared of droplets, the flow rate has been lowered to the desired value.
The droplet breakup, shown in Figure 4.8, is caused by the confinement of the two immiscible flows in the 200 μm wide channel. When an emerging droplet blocks the channel, the upstream pressure rises, so that the liquid interface is pushed downstream and when the neck is thin enough, it will break.

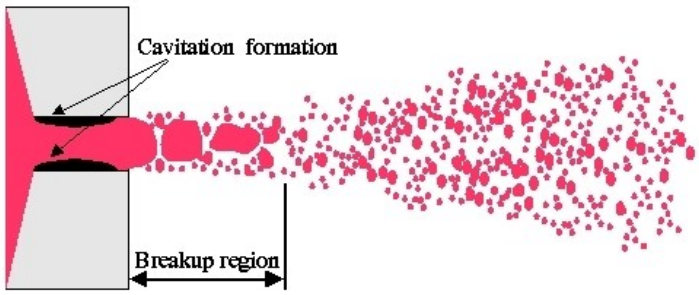

Figure 4.8.*Droplets breakup.*

The frequency of droplets created during the start-up oscillates from an initially high value and then slowly settles towards a stable generation frequency. One unexpected feature of the measurement is an initial increase in the droplet generation frequency, as one might have expected droplets to increase the flow-generated pressure and thus decrease the frequency. The experiments show that the multiphase flow rate decreases slowly from an initially large value. This fluctuation is due to compressibility in the syringe, due to the presence of small air bubbles in it.
To allow the system to reach steady state, all images are taken at least 10 min after adjusting the flow rates.

The steady-state production of drops in the type of device used is mainly characterized by two parameters: the size of each bead and the frequency of generation. While the frequency is directly measured, the size can be estimated from the value of the diameter measured. From the diameter it's possible to calculate the volume of each bead as the product of the visible area of the droplet and the height of the channel, since the discrete phase is shaped similar to a disc.

4.4.2 Water in oil emulsions

4.4.2.1 Effects of the geometry on the droplet formation

Until now there are no general quantitative theories for two-phase flow in a geometry such as the flow-focusing configuration, so different flow conditions have been assessed in two different junction geometries where the main channel contains the dispersed phase (water with 2% of surfactant) and the two side channels contain the continuous phase (light mineral oil).

At first the dispersed phase has been used to fill all the channels (Figure 4.9 and 4.10), at a flow rate of 10 µL/min.

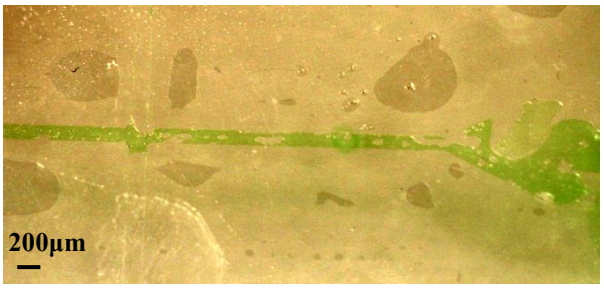

Figure 4.9.*Water flow in the geometry with 90° cross-junction.*

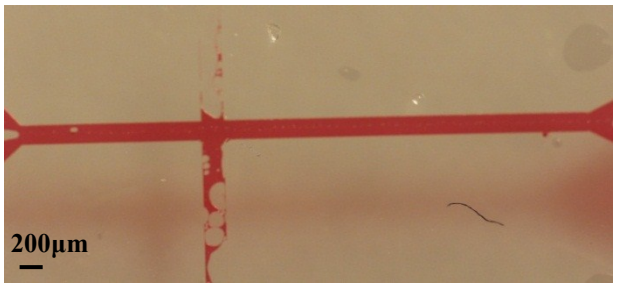

Figure 4.10.*Water flow in the geometry with 45° cross-junction.*

As can be seen from the pictures a monophasic flow is present in the main channel and there are no large differences between the two junctions.

The continuous phase is then dispensed at a flow rate of 20 µL/min, i.e. twice that of the water flow rate. As can be clearly seen in Figure 4.11 and 4.12, the junction of the two immiscible fluids create a laminar flow characterized by a thin water stream in the center of the channel; a thin film of continuous phase liquid, which wets the channels walls, is always between the walls and the dispersed phase liquid. In both the geometries no breakup process occurs when employing these flow rates, and fluids behavior in the microsystem is the same for the two types of junctions.

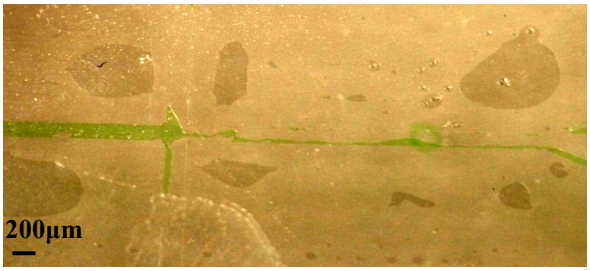

Figure 4.11. *Laminar flow in 90° cross-junction.*

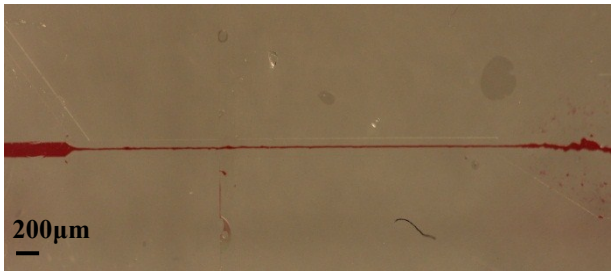

Figure 4.12. *Laminar flow in 45° cross-junction.*

Since no droplets formation was observed with the flow conditions set, the flow rate of the continuous phase is increased to 50 µL/min, 5 times higher than the flow rate in the dispersed phase. The resulting flows are shown in Figure 4.13 and 4.14.

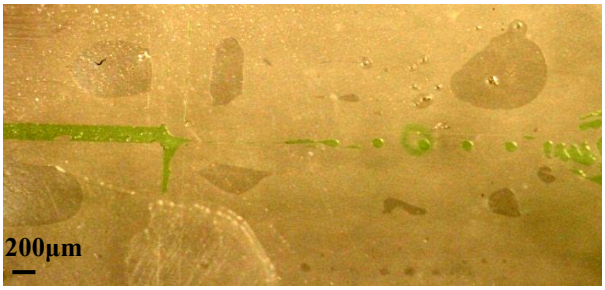

Figure 4.13. *Breakup process in 90° cross-junction.*

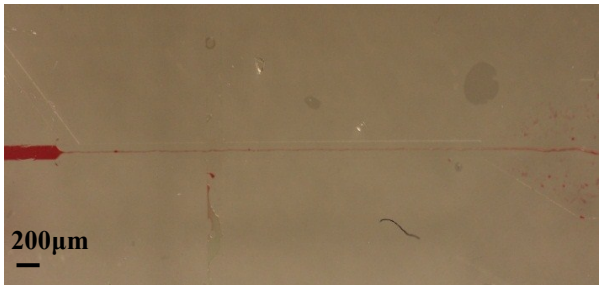

Figure 4.14. *Laminar flow in 45° cross-junction.*

For the 90° cross junction geometry droplets formation occurs, not in the junction section, but 1 cm later and this can be explained by a not homogenous flow from one of the two side channels, due to some inside obstruction in the device. The droplets formed are relatively large and non-uniform.

For the 45° cross junction there is no droplet formation even for higher flow rates; by increasing the flow rate of the oil the stream of water becomes thinner and thinner. At still larger flow rates, the outer flow stabilizes the neck, elongating it further downstream of the junction. When a flow ratio of 100 is reached, the thin stream disappears.

It is clear that the 90° junction geometry is more efficient than the 45° junction geometry, where it is very difficult to form droplets and a precise control and setting of the two flow rates is needed. This result can be explained by the fact that as the flow rate increases, viscous stresses increasingly deform the emerging interface, which forms an elongated conic neck that is narrower than the channel width. Due to the angle of constricting flows, the orthogonal cross junction is more aggressive in breaking this neck. The interface formed is confined by the geometry, which determines the interface curvature; this confinement can prolong the stability of threads as in Figure 4.13.

Since the oil wets the channels walls more readily than the dispersed phase in the 45° cross section it manages to stick to them without interacting with the water stream, while, in the 90°

configuration, the oil is forced to pass through the inner phase, breaking it in small droplets. The wettability is an important parameter for the process since it influences the emulsion morphology and the presence of competitive wetting can lead to erratic two-phase flow patterns.

The 90° junction geometry is more suited for droplet formation since making droplets and tuning the system to reach a stationary condition are easier; for that reason the following experiments for the water in oil emulsions were carried out using that kind of geometry.

4.4.2.2 Effects of the flow rate ratio on the droplets size

Different flow rate ratios (from φ = 5 to φ = 1) have been evaluated to understand how varying the flow rate of the dispersed phase can change the size of the droplets formed.

The flow rate ratio is defined as follow:

$$\varphi = \frac{Q_c}{Q_d}; \tag{4.2}$$

where Q_d and Q_c are the volumetric flow rates of the dispersed phase liquid and of the continuous phase liquid, respectively.

In the experiments carried out the flow rate of the continuous phase has been set to 20 μL/min, while the other has been varied from 20 to 4 μL/min. The diameter of the droplets has been calculated as the mean value of 20 diameter measured for each experiment.

The drop flow rate ratios versus the droplets diameters for the different flow conditions are reported in Figure 4.15.

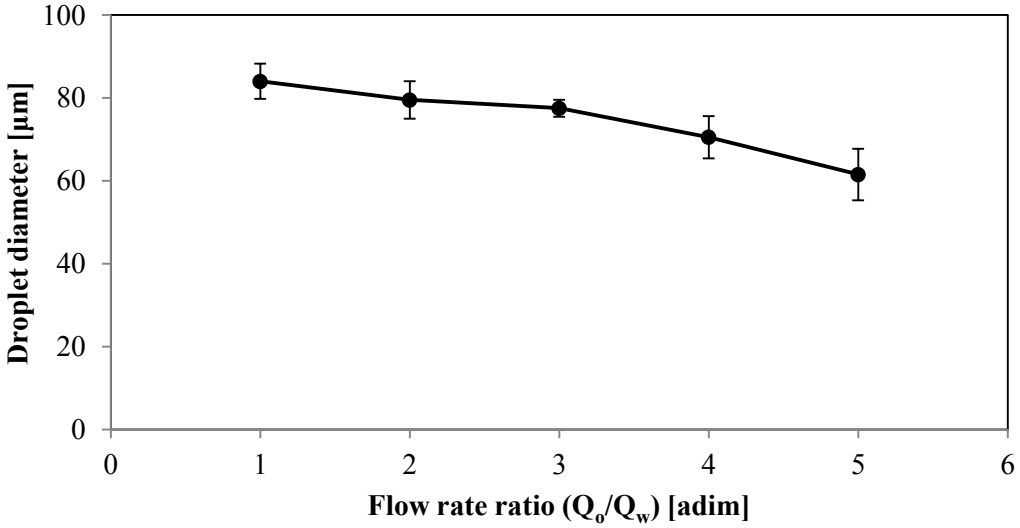

Figure 4.15. *Droplet diameter versus the flow rate ratio.*

In all the cases evaluated the droplets generated are of the same order in size as the dimension of the channels (device size) and their diameter decreases by increasing the flow rate ratio, until reaching a minimum value of 60 μm. This lower limit of the droplets size confirms previous studies in this field (*Anna et al.*, 2003; *Lee et al.*, 2009).

By increasing the flow rate ratio above 5, long plugs are observed, with characteristic dimension much longer than the channel width.
However it must be considered that the diameter calculated is an estimated diameter, determined from the projected area of the droplets, which could be affected by some calculation errors due to the difficulty of in-line droplet size analysis.
Since the volume of a spherical droplet is given by $V = 4/3\ \pi R^3$, where R is the radius of the droplet, the volume of the droplet segment can be calculated from the following equation (*Nie et al*., 2008):

$$V_s = \frac{1}{3}\pi h'^2 (3R - h'); \tag{4.3}$$

where h' is the height of the segment. The volume of the disk with height h (h = 2R - h') is so equal to the equation:

$$V_s = \frac{\pi}{12}\left[2D^3 - (D-h)^2(2D+h)\right]; \tag{4.4}$$

where D is equal to the droplets diameter l measured by the imaging software.
The volumes of the droplets formed have been calculated using the equation above (4.4) and the minimum value of volume reached is equal to ~ 88 nL.
The picture shown in Figure 4.16 can give a qualitative indication of the drop size.

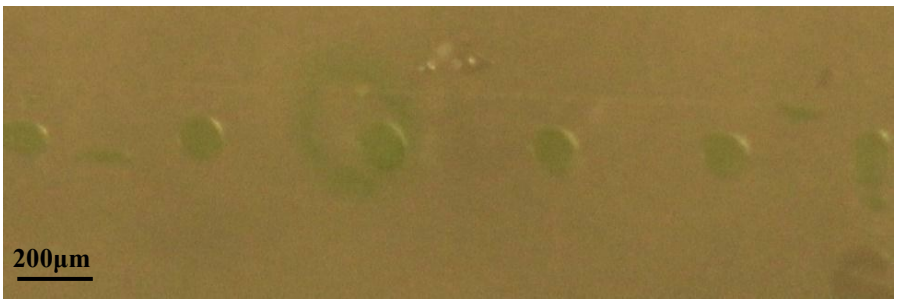

Figure 4.16. *Train of droplets generated.*

4.4.2.3 Effects of the flow rate ratio on the droplet production frequency

The flow rate ratio influences also the frequency of production of the droplets, so, performing the same conditions described in the previous paragraph (4.4.2.2), the value of the frequency (droplets/sec) has been recorded for each experiment. The results are reported in Figure 4.17.

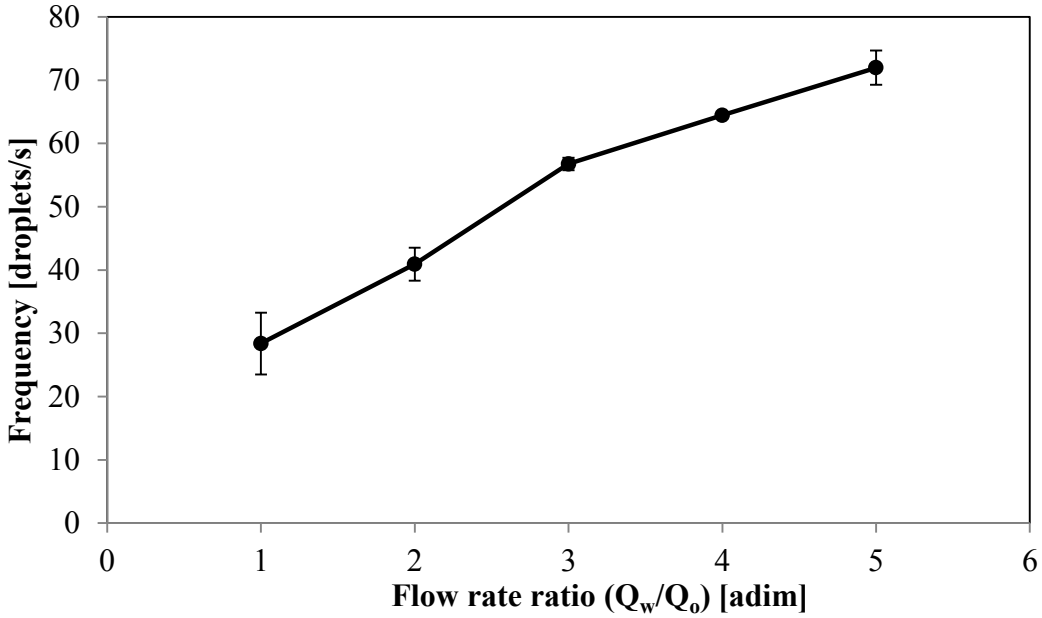

Figure 4.17. *Droplet frequency of production versus the flow rate ratio.*

Figure 4.17 shows how increasing the flow rate ratio increases the frequency of production of the droplets, which will also be smaller in size, as already shown in Fig. 4.15. In order to achieve a high production of the smallest possible droplets, which are best suited for the application desired, high volumetric flow rates of the continuous phase and low volumetric flow rates of the dispersed phase are optimal.

The values of the frequency measured are similar to values found in previous studies, which reported frequencies in the range of 10-1000 droplets/s (*Anna et al*., 2009).

After calculating the distance between the droplets (d) and their speed (u), the frequency measured was verified using the following equation:

$$f = \frac{u}{d}. \tag{4.5}$$

The values of the droplet speed calculated are in the range of ~ 1-100 cm/s and they are close to the speed of the continuous phase in each experiment.

4.4.2.4 Different regimes of flows in the multiphase flow

The key forces involved in droplet breakup are the viscous shear stress, which acts to deform emerging droplet and the surface tension, which resists the deformation, but then aids in necking and pinch-off of the droplets. For that reason the stability of the lab-on-a-chip system depends not only on the flow rates ratio, but also on the inner materials characteristics, especially the interfacial tension (σ) and viscosities (μ) of the liquids used in the microsystem.

The most appropriate dimensionless number to describe droplets formation behavior is the Capillary number (Ca):

$$Ca = \frac{\mu_c Ga}{\sigma} = \frac{\mu_c U}{\sigma}; \tag{4.6}$$

where μ_c is the viscosity of the continuous phase liquid, G is the local shear rate near the droplet, a is the initial radius of emerging droplet, σ is the surface (interfacial) tension and U is the characteristic droplet velocity.

The Capillary number represents the balance between the viscous forces and interfacial tension at the surface of two fluids. Accordingly, the size of droplets changes by capillary number due to viscous force and the interfacial tension.

While flow rate ratio affects the droplet formation behavior significantly, as already shown, the viscosity ratio has a relatively weak impact on the droplet diameter compared to capillary number (Ca), since the flow rate is associated with characteristic velocity of Ca. Therefore the viscosity ratio, defined by equation 4.7, has been considered constant during the experiments:

$$\lambda = \frac{\mu_d}{\mu_c}; \tag{4.7}$$

where μ_d and μ_c are the viscosities of the dispersed phase liquid and of the conituous one, respectively.

Since the droplet diameter is a function of the Ca and of the relative flows of the two immiscible fluids, some experiments for different values of Ca have been conducted to understand the relationship between Ca and the size of the droplets. The results are reported in Figure 4.18.

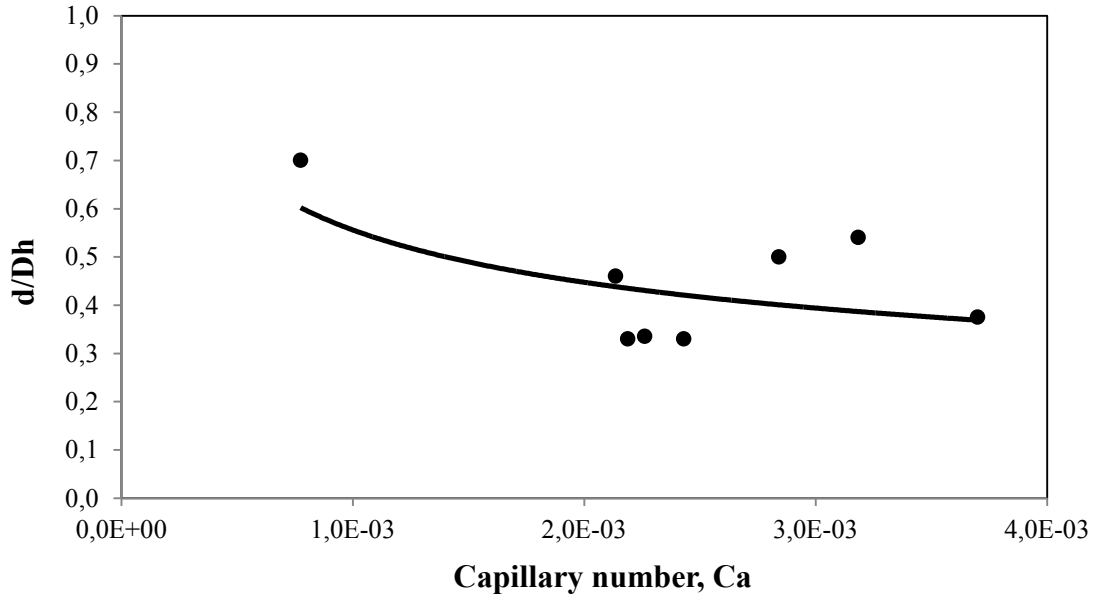

Figure 4.18. *Effect of Ca on the droplets size.*

In Figure 4.18 the droplet diameter has been made dimensionless by dividing it for D_h, which is the hydraulic diameter of the channels, defined by the following equation:

$$D_h = \frac{4S}{P}; \tag{4.8}$$

where *S* is the cross area of the channels, while *P* is the wet perimeter.
From Figure 4.17 it has been found that the relationship between the dimensionless droplets diameter and Ca is the following:

$$\frac{d}{D_h} \propto Ca^{-1/3}; \tag{4.9}$$

so by increasing the droplets speed their size tends to decrease, provided that the viscosity of the continuous phase and the interfacial tension are kept constant.
Different values of Ca imply also different regimes of flows, as shown in the pictures in Figure 4.19.

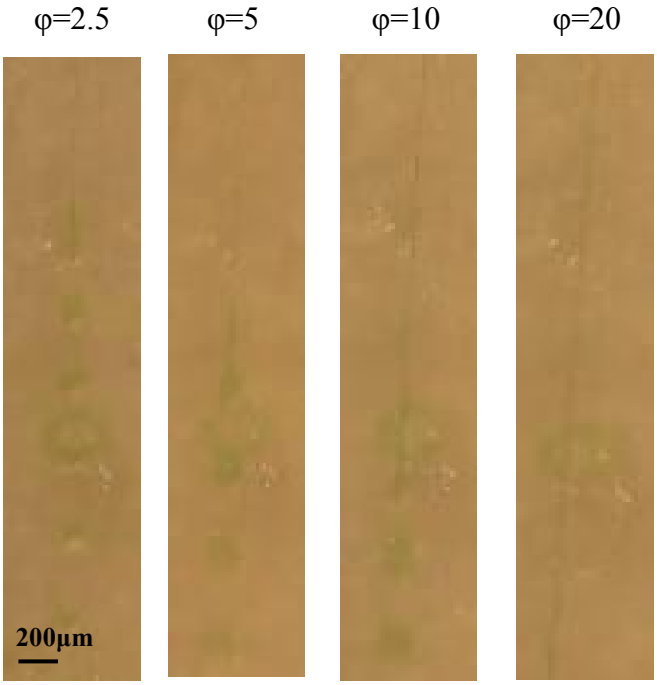

Figure 4.19. *Different regimes of flow for water in oil emulsions.*

At low values of Ca (low values of flow rate ratio) the flow regime can be termed ″squeezing″, the breakup is not driven by capillary forces, it's near to the junction and small droplets move along centerline as particles. When the flow rate of the continuous phase increases, the capillary instabilities lead to breakup, further downstream, and the regime of flow is called ″dripping″. If the flow rate ratio is increased even more ($Q_w << Q_o$) long thin threads are formed, the viscous stresses become dominant and the regime of flow is termed ″viscous jetting″.

4.4.3 Oil in water emulsions

Since the microfluidic platform has been developed for a double emulsion process, needed for the biomedical application of the device, also oil in water emulsion have been investigated,

using the 45° junction geometry and carrying out the same experiments done for the water in oil emulsions.

4.4.3.1 Effects of the flow rate ratio on the droplets size

In Figure 4.20 it is represented how the flow rate ratio influences the droplets size.

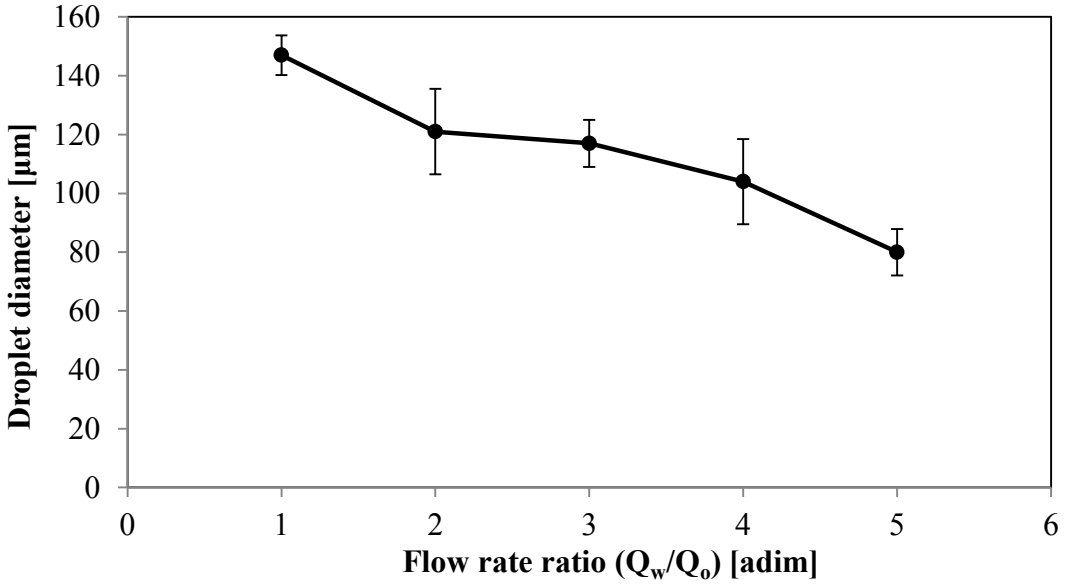

Figure 4.20. *Droplet diameter estimated versus the flow rate ratio.*

As for the water in oil emulsions, when increasing the flow rate ratio the diameter of the droplets decreases. The minimum value of the diameter measured is higher than the one for w/o emulsion and it is equal to ~ 80 µm. The minimum volume calculated, through equation 4.2, is of 265 nL, which is around three times the minimum volume calculated for w/o emulsions.

4.4.3.2 Effects of the flow rate ratio on the droplet production frequency

In Figure 4.21 the influence of the flow rate ratio on the droplets frequency of production is represented.

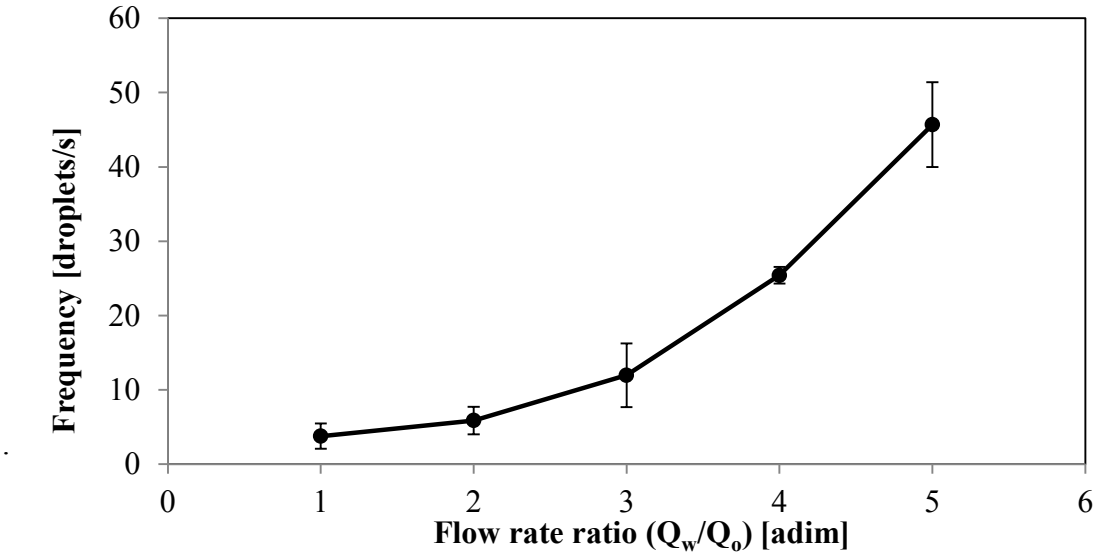

Figure 4.21. *Droplet frequency of production versus the flow rate ratio.*

As for the w/o emulsions, increasing the flow rate ratio increases the frequency of droplets production. In order to get small droplets at high frequency, a high volumetric flow rate of the continuous phase and low ones of the dispersed phase are recommended.

4.4.3.3 Different regimes of flows in the multiphase flow

The relationship between the Capillary number (Ca) and the droplets diameter has been investigated also for the o/w emulsions and the results are reported in Figure 4.22.

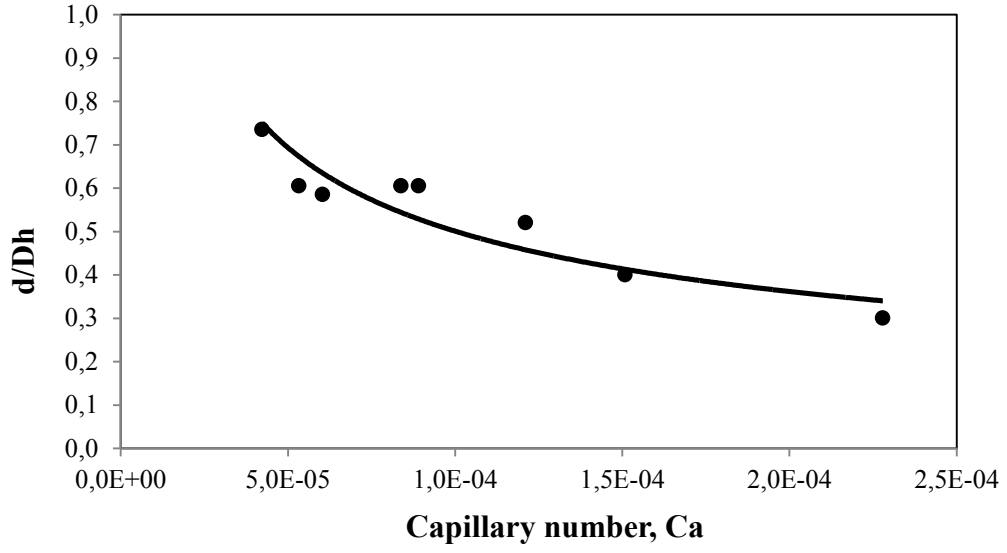

Figure 4.22. *Effect of Ca on the droplets size.*

Like in w/o emulsions the diameter decreases when Ca increases, but the speed of this reduction is different and it can be described by the following proportion:

$$\frac{d}{D_h} \propto Ca^{-1/2}; \tag{4.10}$$

so by increasing the droplets speed their size tends to decrease more than in w/o emulsions, given that the viscosity of the continuous phase and the interfacial tension are constant.
Different regimes of flows for different flow rate ratios are shown in Figure 4.23, where φ represents the flow rate ratio. The regimes observed are equal to the ones observed for w/o emulsions. A difference is observed for high flow rate ratios, where for o/w emulsions the small droplets formed don't move in the middle of the channel, but they try to stay near the walls. This effect is due to the hydrophobic properties of the channels walls.

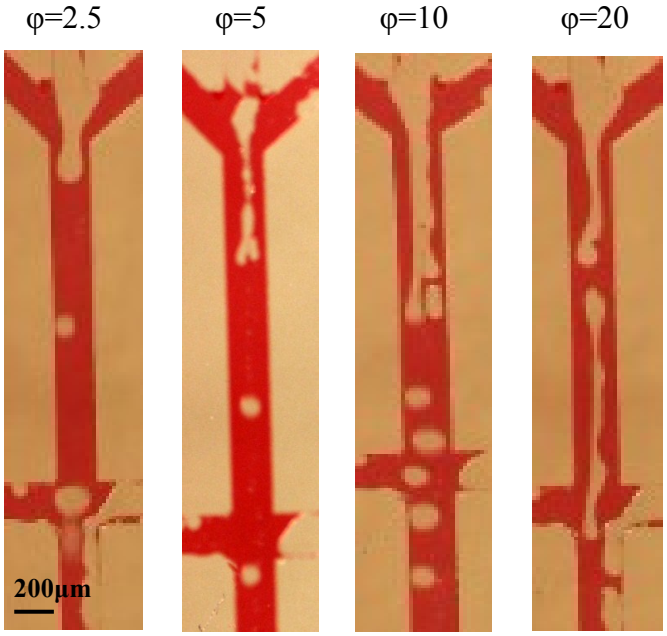

Figure 4.23. *Different regimes of flow for oil in water emulsions.*

Until φ = 5 a squeezing regime is observed; for φ = 10 a dripping regime is present and after φ = 20 the jetting mode starts and no more droplets are formed.

4.4.3.4 Narrow size distribution for w/o and o/w emulsions

To check the uniformity of the multiphase system a particle size distribution has been represented in Figure 4.24 and Figure 4.25, for both w/o and o/w emulsions. The diameters represented have been measured setting a flow rate ratio equal to 5 and with a flow rate of the dispersed phase of 5 µL/min.

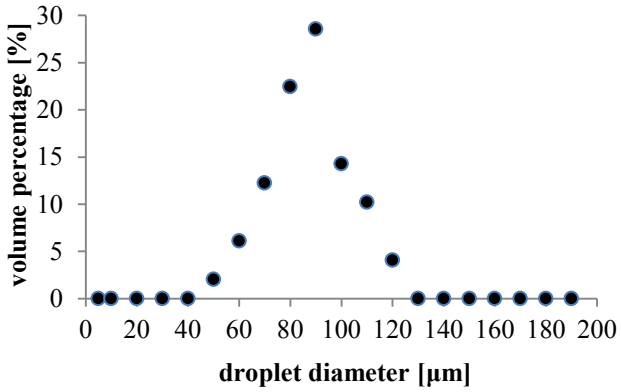

Figure 4.24. *Narrow size distribution for w/o emulsions.*

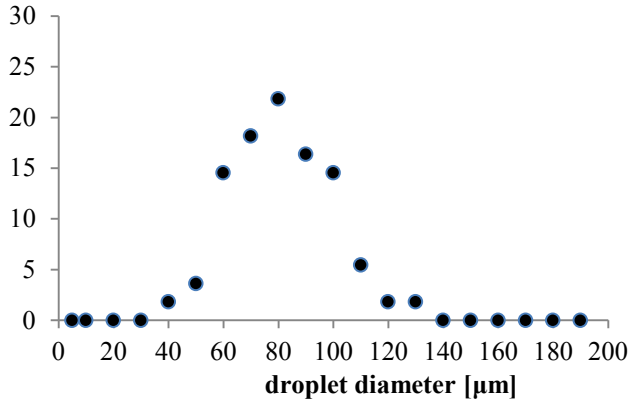

Figure 4.25. *Narrow size distribution for o/w emulsion.*

From the two figures it is highlighted that the droplets are quite uniform, included in a range of 50-120 µm for w/o emulsions and of 40-130 µm for o/w emulsions; in both cases the droplets size is similar to the channel size.

The droplets size for w/o emulsions shows a narrower distribution than o/w emulsions.

Both emulsions process seem suitable for the application desired and all the experiments have confirmed the potential efficiency of this microsystem for the production of a uniform train of small droplets at high frequency.

Conclusions

In this thesis work a microfluidic platform for emulsion processes has been designed, developed and tested using water and mineral oil as model fluids. The material used for making the microdevice is a novel polymeric material, Off-Stoichiometry Thiol-Ene/Epoxy (OSTE(+)). This material allows for a UV-curing system for achieving surface modifications and its good bonding properties offer many advantages, like a low level of energy consumption and a fast curing rate, that can be of great interest for industrial applications as well. Moreover the fabrication step can be carried out in a batch and this is an advantage in terms of production rate.

Characterization's conducted on the microsystem fabricated have shown the efficiency of the hydrophobic surface modification technique employed, a good leak tight bonding between the two OSTE (+) layers which form the device and no clogging in the microchannels.

The experimental results have underlined that the flow rate ratio between the two fluids employed is the most important variable in the emulsion process. The flow rate ratio influences the regime of flow, the size, the speed and the frequency of production of the droplets. In order to get a high production frequency of uniform droplets with sizes comparable with the channels dimensions, high flow rate ratio between the continuous phase and the dispersed phase are needed. The investigation on the geometry of the channels junction has shown that the better solution for the breakup process in the emulsion process is a 90° cross junction.

Further studies are suggested before carrying out the double emulsion process for cell encapsulation in the microfluidic device.

Since the surface tension plays an important role in the droplets breakup, its effect on the process should be evaluated and different concentrations of surfactant in the water phase should be tested. Adding a proper surfactant can improve stability of the droplets and decrease the size of droplets because the surfactant molecules reduce the interfacial tension between the fluids in each droplet, avoiding the undesirable coalescence among droplets.

The channels design could be improved by adding an orifice just after the channels junction, in order to speed the breakup process.

Instead of using water in the emulsions, Polyethylene Glycol (PEG) should be employed, since it is a suitable material for core in the desired core shell geometry.

Finally some fluidodynamic simulation could help to set the volumetric flow of the two fluids in the emulsion process and to confirm the experimental results.

References

Allen, T.M. and Cullis, P.R. (2004). Drug delivery systems: entering the mainstream. *Science*, **303**, 1818-1822.

Becker, P. (1965). *Emulsions: theory and practice*. Rheinhold Publ. Corp., New York (USA).

Becker, H. and Gärtner, C. (2007). Polymer microfabrication technologies for microfluidic systems. *Analytical and Bioanalytical Chemistry*, **390**, 89-111.

Carioscia, J. A. et al. (2007). Evaluation and control of thiol-ene/thiol-epoxy hybrid networks. *Polymer*, **48**, 1526-1532.

Carlborg, C. F. et al. (2011). Beyond PDMS: off-stoichiometry thiol–ene (OSTE) based soft lithography for rapid prototyping of microfluidic devices. *Lab on a Chip*, **11**, 3136-3147.

Chang, C. C. et al. (2008). Hydrodynamic focusing effect on two-unmixed-fluid in microchannels. *International Journal of Nonlinear Sciences and Numerical Simulation*, **9**, 213-221.

Chang, T. M. S. (1957). *Hemoglobin corpuscles*. Report of a research, McGill University, 1-25, Montreal (Canada).

Clanet, C. and Lasheras J. C. (1999). Transition from dripping to jetting. *Journal of Fluid Mechanics*, **383**, 307-326.

Cubaud, T. et al. (2005). Two-phase flow in microchannels with surface modifications. *Fluid Dynamics Research*, **38**, 772–786.

De Groot, M. et al. (2003). Effective removal of alginate-poly-L-lysine microcapsules from pancreatic islets by use of trypsin-EDTA. *Journal Of Biomedical Materials Research Part A*, **67A**, 679-683.

Dreyfus, R. et al. (2003). Ordered and disordered patterns in two-phase flows in microchannels. *Physical Review Letters*, **90**.

Goh, C. S. et al. (2009). Adhesive bonding of polymeric microfluidic devices. *Electronics Packaging Technology Conference*, 9-11 December ´09, 11th edition, Singapore.

Goubault, C. et al. (2001). Shear rupturing of complex fluids: application to the preparation of monodisperse W/O/W double emulsions. *Langmuir*, **17**, 5184-5188.

Hahn, S.K. et al. (2004). Anti-inflammatory drug delivery from hyaluronic acid hydrogels. *Biomaterials*, **15**, 1111-1119.

Hoffmann, E. K. et al. (1993). Cell volume regulation: intracellular transmission. *Adv. Comp. Env. Physiol*, **14**, 187-248.

Hwang, D. K. et al. (2008). Microfluidic-based synthesis of non-spherical magnetic hydrogel microparticles. *Lab on a Chip*, **8**, 1640-1645.

Leach, J. B. and Schmidt, C. E. (2005). Characterization of protein release from photocrosslinkable hyaluronic acid-polyethylene glycol hydrogel tissue engineering scaffolds. *Biomaterials*, **26**, 125-135.

Lee, D. and Weitz, D.A. (2008). Double emulsion-templated nanoparticle colloidosomes with selective permeability. *Advanced Materials*, **20**.

Lissant, K. J. (1974). *Emulsions and emulsion technology*. M. Dekker, New York (USA).

Löhr, M. et al. (2001). Microencapsulated cell-mediated treatment of inoperable pancreatic carcinoma. *The Lancet*, **357**, 1591-1592.

Lowe, A. B. (2009). Thiol-ene ″click″ reactions and recent applications in polymer and materials synthesis. *Polymer Chemistry*, **1**, 17-36.

Murua, A. et al. (2008). Cell microencapsulation technology: towards clinical application. *Journal of Controlled Release*, **132**, 76-83.

Nguyen, K.T. and West, J.L. (2002). Photopolymerizable hydrogels for tissue engineering applications. *Biomaterials*, **23**, 4307-4314.

Nie, Z. et al. (2008). Emulsification in a microfluidic flow-focusing device: effect of the viscosities of the liquids. *Microfluid Nanofluid*, **5**, 585-594.

Orive, G. et al. (2003). Cell microencapsulation technology for biomedical purposes: novel insights and challenges. *Trends in Pharmacological Sciences*, **24**, 207-210.

Orive, G. et al. (2005). Micro and nano drug delivery systems in cancer therapy. *Cancer Therapy*, **3**, 131-138.

Rabold, M. et al. (2009). Surface-energy characterization of full-wafer bonds using the concealed blister test method. *Electrochemical and Solid-State Letters*, **12**, H176-H178.

Reddy, S. K. et al. (2004). Living radical photopolymerization induced grafting on thiol–ene based substrates. *Journal of Polymer Science*, **43**, 2134-2144.

Saharil, F. et al. (2012). Biocompatible ″click″ wafer bonding for microfluidic devices. *Lab on a Chip*, DOI: 10.1039/C2LC21098C.

Saharil, F. et al. (2012). Dry transfer bonding of porous silicon membranes to OSTE (+) polymer microfluidic devices. Presented at *MEMS*, Paris, France, 29 January - 2 February 2012.

Seemann, R. et al. (2012). Droplet based microfluidics. *Report of Progress in Physics*, **75**, 016601.

Segura, T. et al. (2005). Crosslinked hyaluronic acid hydrogels: a strategy to functionalize and pattern. *Biomaterials*, **26**, 359-371.

Setu, P. and Mastrangelo, C. H. (2003). Cast epoxy-based microfluidic systems and their application in biotechnology. *Sensor and actuators*, **98**, 337-346.

Stone, H.A. et al. (2004). Microfluidics toward a lab-on-a-chip. *Fluid Mechanics*, **36**, 381-411.

Vallin, O. et al. (2005). Adhesion quantification methods for wafer bonding. *Materials Science and Engineering*, **50**, 109–165.
Williams, J.R. et al. (1999). Predicting cancer rates in astronauts from animal carcinogenesis studies and cellular markers. *Mutation Research*, **430**, 255-269.
Witkop, B. (1999). Paul Elrich and his magic bullets. *Proceedings of the American Philosophical Society*, **143**, 540-557.
Woodward, R. P. (1999). Contact angle measurements using the drop shape method. *First ten Angstrom*, 1-8.
Ye, C. et al. (2010). Ceramic microparticles and capsules via microfluidic processing of a preceramic polymer. *Journal of the Royal Society Interface*, **7**, 461-473.

Acknowledgments

This project would not have been possible with the contribution of several people, who, in different ways, have contributed to its completion.
First of all I truly want to thank my supervisor here in Sweden, dr. Tommy Haraldsson: with his patience he has always answered to all my questions; his optimistic view of things and funny comments on the experimental work have helped me not to lose hope in what I was doing.
Thanks to my Italian supervisor, prof. Nicola Elvassore, for having suggested me to contact this group at KTH, for having always supported me in my desire to have an experience abroad and in my project here.
Thanks to Mikael, Frederik, Farizah and especially Niklas, for their numerous lab suggestions and for their interest in my work.
Thanks to Wouter Van der Wijngaart for having accepted me in his group and for making such a good atmosphere at MST.

Thanks to Lilli&Roby for having been my best friends, flat mates, schoolmates and whatever for so many years. I feel very lucky to have you near me in each step of my life.
Thanks to Giacomo, Damiano, Enrico and Vanessa, for all your support, although we all are in different parts of the world. Thanks for the long skype conversations, for having always helped me when needed and for having been the best projects mates ever. I can't think about my university years without you (..and of course JB, the fruit of the three, start-cup e our caf group).
Thanks to all the Gamla Stan drinkers for having made my Erasmus in Stockholm such an awesome experience.
Barcelona, Lappis and our trips have made me really enjoy this period of studies abroad.
Thanks to Fede, Jenni and Emi for all the great moments spent together.
Thanks to Laura for her wise suggestions, for making me doing my best in everything and for believing so much in my abilities.

Last but not the least, thanks to my family, especially my father, and my sister, for motivating me, for saying always the truth about my work and for having shared with me so many hours of studying (in different rooms!).